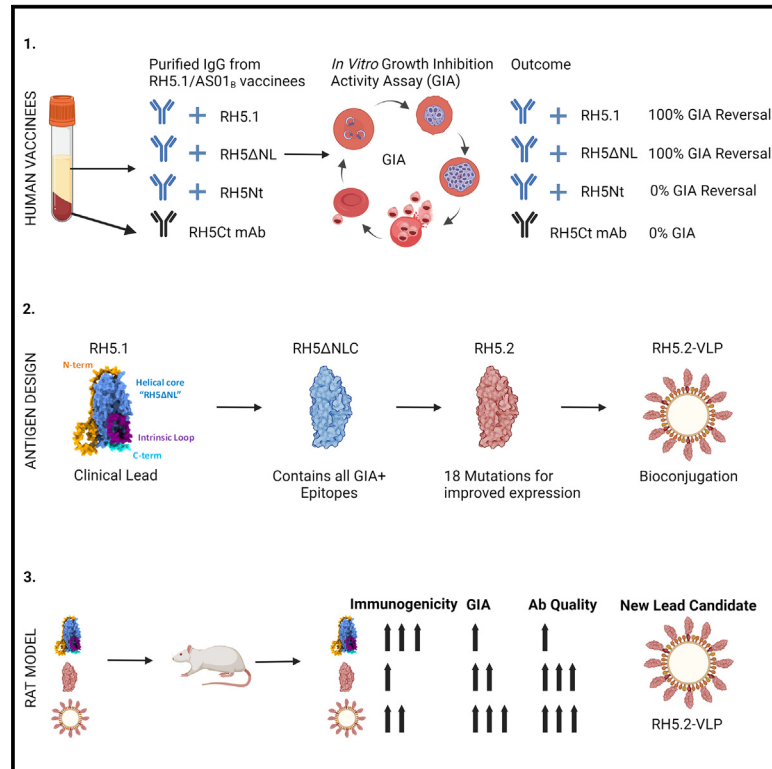


Preclinical development of a stabilized RH5 virus-like particle vaccine that induces improved antimalarial antibodies

Graphical abstract



Authors

Lloyd D.W. King, David Pulido, Jordan R. Barrett, ..., Mark R. Howarth, Sumi Biswas, Simon J. Draper

Correspondence

simon.draper@bioch.ox.ac.uk

In brief

King et al. describe an improved blood-stage malaria vaccine candidate, RH5.2-VLP, that outperforms the current clinical lead, RH5.1/Matrix-M, in rats. They demonstrate improved qualitative growth inhibitory antibody responses following deletion of disordered regions of RH5 and report the highest antibody-mediated *in vitro* growth inhibitory activity in RH5.2-VLP/Matrix-M-immunized rats.

Highlights

- Inhibitory antibodies from RH5.1/AS01_B vaccinees target the RH5 α -helical core
- A truncated and thermostabilized RH5.2 immunogen induces more potent antibodies
- Bioconjugation of RH5.2 to VLPs enhances antibody immunogenicity in rodents
- RH5.2-VLP/Matrix-M induces highest functional antimalarial antibodies in rats



Article

Preclinical development of a stabilized RH5 virus-like particle vaccine that induces improved antimalarial antibodies

Lloyd D.W. King,^{1,2,3} David Pulido,³ Jordan R. Barrett,^{1,2,3} Hannah Davies,^{1,2,3} Doris Quinkert,^{1,2,3} Amelia M. Lias,^{1,2,3} Sarah E. Silk,^{1,2,3} David J. Pattinson,³ Ababacar Diouf,⁴ Barnabas G. Williams,^{1,2,3} Kirsty McHugh,^{1,2,3} Ana Rodrigues,^{1,2} Cassandra A. Rigby,^{1,2} Veronica Strazza,^{1,2} Jonathan Suurbaar,^{3,5} Chloe Rees-Spear,^{3,6} Rebecca A. Dabbs,³ Andrew S. Ishizuka,³ Yu Zhou,³ Gaurav Gupta,³ Jing Jin,³ Yuanyuan Li,³ Cecilia Carnrot,⁷ Angela M. Minassian,^{1,2,3,8} Ivan Campeotto,¹ Sarel J. Fleishman,⁹ Amy R. Noe,^{10,13} Randall S. MacGill,¹¹ C. Richter King,¹¹ Ashley J. Birkett,¹¹ Lorraine A. Soisson,¹² Carole A. Long,⁴ Kazutoyo Miura,⁴ Rebecca Ashfield,^{1,2,3} Katherine Skinner,^{1,2,3} Mark R. Howarth,^{1,14} Sumi Biswas,³ and Simon J. Draper^{1,2,3,8,15,*}

¹Department of Biochemistry, University of Oxford, Dorothy Crowfoot Hodgkin Building, OX1 3QU Oxford, UK

²Kavli Institute for Nanoscience Discovery, Dorothy Crowfoot Hodgkin Building, University of Oxford, OX1 3QU Oxford, UK

³The Jenner Institute, University of Oxford, Old Road Campus Research Building, OX3 7DQ Oxford, UK

⁴Laboratory of Malaria and Vector Research, NIAID/NIH, Rockville, MD 20852, USA

⁵West African Centre for Cell Biology of Infectious Pathogens, University of Ghana, Accra LG 54, Ghana

⁶London School of Hygiene and Tropical Medicine, WC1E 7HT London, UK

⁷Novavax AB, Kungsgatan 109, 753 18 Uppsala, Sweden

⁸NIHR Oxford Biomedical Research Centre, Oxford, UK

⁹Department of Biomolecular Sciences, Weizmann Institute of Science, Rehovot, Israel

¹⁰Leidos Life Sciences, Frederick, MD, USA

¹¹Center for Vaccine Innovation and Access, PATH, Washington, DC 20001, USA

¹²USAID, 1300 Pennsylvania Avenue NW, Washington, DC 20004, USA

¹³Present address: Latham BioPharm Group, Elkridge, MD, USA

¹⁴Present address: Department of Pharmacology, University of Cambridge, Tennis Court Road, CB2 1PD Cambridge, UK

¹⁵Lead contact

*Correspondence: simon.draper@bioch.ox.ac.uk

<https://doi.org/10.1016/j.xcrm.2024.101654>

SUMMARY

Plasmodium falciparum reticulocyte-binding protein homolog 5 (RH5) is a leading blood-stage malaria vaccine antigen target, currently in a phase 2b clinical trial as a full-length soluble protein/adjuvant vaccine candidate called RH5.1/Matrix-M. We identify that disordered regions of the full-length RH5 molecule induce non-growth inhibitory antibodies in human vaccinees and that a re-engineered and stabilized immunogen (including just the alpha-helical core of RH5) induces a qualitatively superior growth inhibitory antibody response in rats vaccinated with this protein formulated in Matrix-M adjuvant. In parallel, bioconjugation of this immunogen, termed “RH5.2,” to hepatitis B surface antigen virus-like particles (VLPs) using the “plug-and-display” SpyTag-SpyCatcher platform technology also enables superior quantitative antibody immunogenicity over soluble protein/adjuvant in vaccinated mice and rats. These studies identify a blood-stage malaria vaccine candidate that may improve upon the current leading soluble protein vaccine candidate RH5.1/Matrix-M. The RH5.2-VLP/Matrix-M vaccine candidate is now under evaluation in phase 1a/b clinical trials.

INTRODUCTION

Over the past two decades, the number of deaths from malaria, caused by the *Plasmodium falciparum* parasite, has been steadily declining due to the improved deployment of antimalarial tools. However, the success of malaria control measures requires sustained investment, which is expensive and threatened by the emergence of drug and insecticide resistance. Moreover, evidence suggests progress has stalled in recent

years, with malaria cases and deaths rising since 2019.¹ Hence, there remains an urgent need for the development of transformative new tools, including highly efficacious and durable malaria vaccines, to complement and/or replace current malaria prevention public health measures. Substantial recent progress has been made in this area, with the RTS,S/AS01 (Mosquirix) and R21/Matrix-M subunit vaccines (that both target the circumsporozoite protein [CSP] on the liver-invasive sporozoite stage of *P. falciparum*) showing efficacy against clinical malaria in young



African children.^{2,3} However, efficacy wanes over time, and if a single sporozoite slips through the net of protective immunity and infects the liver, then the subsequent disease-causing blood stage of infection is initiated. Seasonal vaccination has been demonstrated to be highly efficacious in phase 3 trials, with RTS,S/AS01 (Mosquirix) non-inferior to seasonal malarial chemoprophylaxis, which has been associated with approximately 75% efficacy^{4–6}; however, annual vaccination is expensive and a major burden on already stretched health systems.⁷ Vaccination against the blood-stage merozoite, aiming to prevent erythrocyte invasion and the clinical manifestation of malaria disease, represents an alternative and complementary approach. Moreover, the combination of a blood-stage anti-merozoite vaccine with existing anti-sporozoite vaccines is currently regarded as a leading future vaccination strategy to achieve higher and more durable efficacy.⁸

Merozoite invasion of human erythrocytes occurs rapidly and in a complex multistep process requiring numerous parasite ligand-host receptor interactions. Historic blood-stage vaccine candidates struggled because many of these parasite ligands are highly polymorphic and the interactions they mediate are redundant.⁹ However, the identification of the reticulocyte-binding protein homolog 5 (RH5)¹⁰ has renewed vigor in the *P. falciparum* blood-stage vaccine field over the last decade.⁸ RH5 is an essential, highly conserved, and antibody-susceptible antigen delivered to the parasite surface in a pentameric protein complex^{11–13} where it binds to host basigin/CD147.¹⁴ This receptor-ligand interaction is critical for parasite invasion¹⁵ and underlies the human host tropism of *P. falciparum*,¹⁶ and vaccination of *Aotus* monkeys with RH5 conferred significant *in vivo* protection against a stringent blood-stage *P. falciparum* challenge.¹⁷ These preclinical data supported the onward progression of RH5-based vaccine candidates to the clinic, with four early-phase clinical trials now completed in the UK or Tanzania; each of these studies utilized vaccines that deliver the full-length RH5 molecule (RH5_FL) using either a viral-vectored platform^{18,19} or a recombinant protein called RH5.1²⁰ formulated in AS01_B adjuvant from GSK²¹ or Matrix-M adjuvant from Novavax.²² These vaccines have shown acceptable safety and reactogenicity profiles, with the highest levels of antibody observed when using the protein-in-adjuvant formulations^{21,22} and/or when vaccinating Tanzanian infants or children as opposed to UK or Tanzanian adults.^{19,22} The RH5.1/Matrix-M vaccine candidate has since progressed to a phase 2b field efficacy trial in 5- to 17-month-old children in Burkina Faso ([ClinicalTrials.gov](https://clinicaltrials.gov/ct2/show/study/NCT05790889) NCT05790889).

These vaccines have also induced serum immunoglobulin G (IgG) antibodies in humans that mediate functional growth inhibition activity (GIA) against *P. falciparum* *in vitro*. Notably, despite differences in the quantity of anti-RH5 serum IgG induced, the functional quality of the anti-RH5 human IgG is comparable,^{19,22} i.e., these vaccines achieve the same amount of GIA *in vitro* per unit of anti-RH5 antibody, consistent with them all encoding immunogens based on RH5_FL. Importantly, GIA has also been shown to correlate with vaccine-induced efficacy against experimental *P. falciparum* blood-stage challenge of both *Aotus* monkeys¹⁷ and UK adults,²¹ with this mechanism of protection subsequently validated by passive transfer of anti-RH5 monoclonal antibody (mAb) in *Aotus* monkeys²³ and a humanized mouse

model.²⁴ However, despite this progress, the overall quantity of anti-RH5_FL IgG associated with protection in the *Aotus* monkey model was high, requiring >300 μg/mL,¹⁷ while vaccination of UK adults with RH5.1/AS01_B achieved ~100 μg/mL.²¹ An improved vaccine in adults will thus likely necessitate a minimum 3-fold improvement in terms of the quantitative and/or qualitative RH5-specific antibody response. We therefore sought here to develop an RH5-based vaccine candidate that could substantially outperform the current clinical lead vaccine candidate, RH5.1/Matrix-M. To do this, we explored rational re-design of the RH5 immunogen based on serological analyses of the anti-RH5.1 IgG from clinical trials and improved the delivery of RH5 using a virus-like particle (VLP) platform. In the case of the latter, given the well-described challenges of recombinant RH5 protein expression and our unsuccessful attempts to express existing RH5 immunogens as a direct genetic fusion to various VLP platforms, we decided to test a “plug-and-display” strategy using SpyTag-SpyCatcher bioconjugation technology.^{25,26} We also elected to use the hepatitis B surface antigen (HBsAg) VLP scaffold,²⁷ given the extensive safety track record of the hepatitis B vaccine in humans²⁸ and to align the delivery platform with that used for delivery of the CSP antigen by both RTS,S and R21^{2,3}.

RESULTS

Vaccine-induced human anti-RH5 growth inhibitory antibodies target RH5ΔNLC

We previously assessed the RH5.1/AS01_B vaccine candidate in healthy malaria-naïve UK adults, using a variety of dosing and immunization regimens.²¹ The RH5.1 protein was manufactured in a *Drosophila* Schneider 2 (S2) stable cell line system and comprises the whole ~60 kDa RH5-soluble molecule with four sites of potential N-linked glycosylation removed.²⁰ This molecule therefore includes the structured alpha-helical core of RH5 (termed “RH5ΔNLC”) and the predicted regions of disorder: the long N-terminal region, intrinsic loop, and small C terminus (Figure 1A). The structure of the α-helical core protein (including the small C terminus but lacking the N terminus and intrinsic loop, known as “RH5ΔNL”) was previously reported.²⁹ Human serum samples, collected after three immunizations with RH5.1/AS01_B, were all positive for IgG by ELISA against the recombinant full-length RH5.1, RH5 N terminus (RH5-Nt), and RH5ΔNL proteins. Responses were comparable and did not differ significantly by vaccine dose or delivery regimen (Figure 1B). Sera were also tested by ELISA against a linear peptide array spanning the RH5.1 antigen sequence. Responses were clearly detectable across all the regions of predicted protein disorder (N-terminal region, intrinsic loop, and C terminus), confirming these contain linear antibody epitopes that appear largely absent in the α-helical core regions (Figure 1C). Vaccine-induced anti-RH5.1 serum IgG responses thus reacted across the whole molecule, including regions comprising both linear and conformational epitopes.

We next assessed whether IgG antibodies targeting these different structural regions contribute to functional growth inhibition of *P. falciparum* parasites *in vitro* by first using an “antigen-reversal” GIA assay. As expected, inclusion of recombinant RH5.1 protein in the GIA assay could completely reverse all GIA

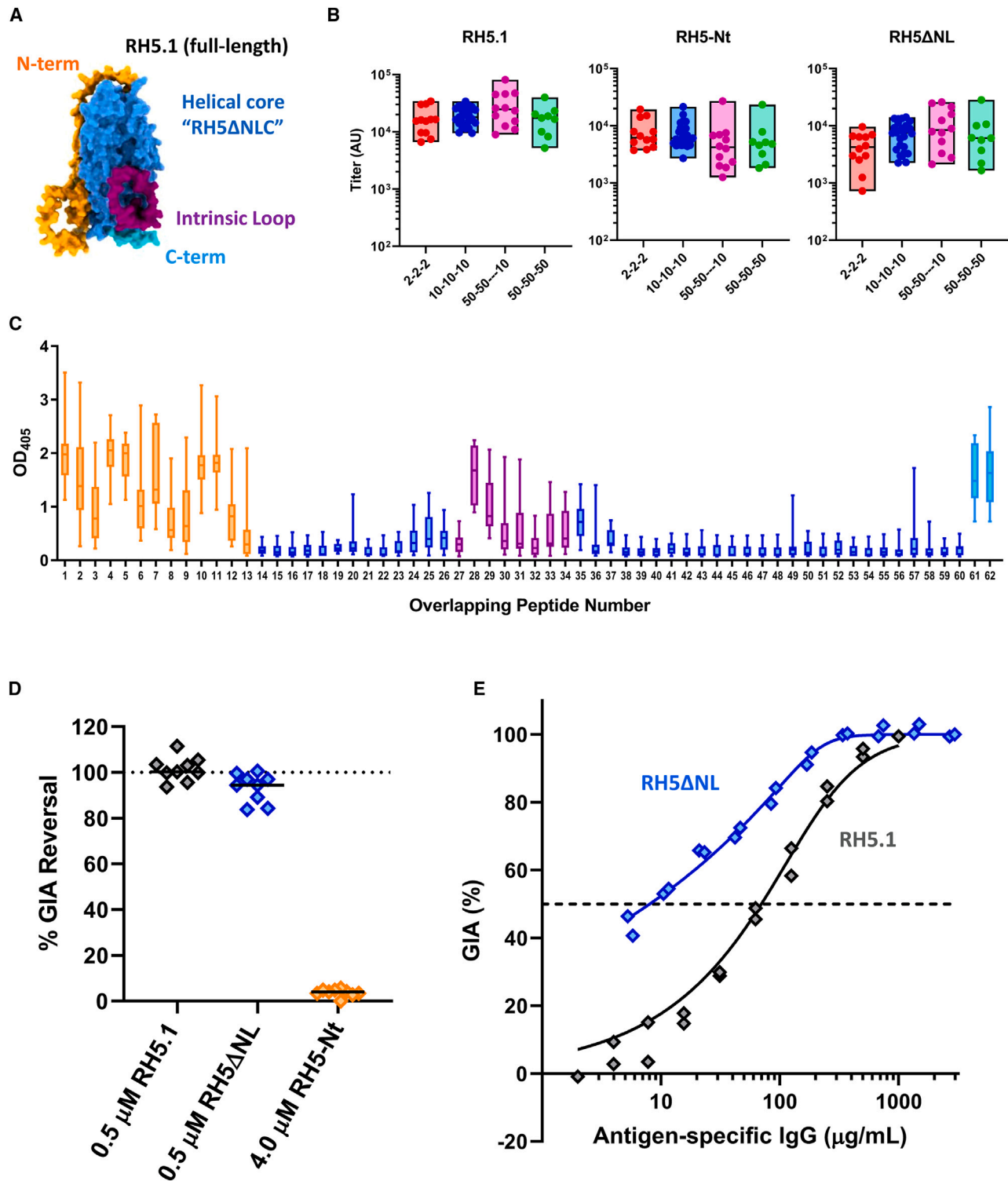


Figure 1. Assessment of vaccine-induced human anti-RH5.1 antibody targets

(A) AlphaFold model (#AF-Q8IFM5-F1) of the full-length RH5 molecule on which the RH5.1 protein (amino acids [aa] E26-Q526) vaccine²⁰ was based. The structured alpha-helical core ("RH5ΔNLC") is shown in light blue, while the regions of predicted disorder include the linear N terminus (RH5-Nt; aa E26-Y139; orange), the intrinsic loop (aa N248-M296; purple), and small C terminus (aa D507-Q526; cyan).²⁹

(B) Serum IgG antibody titers in RH5.1/AS01_B vaccinees as measured by ELISA against recombinant RH5.1, RH5-Nt, and RH5ΔNL proteins in arbitrary units (AU). Vaccinees received three doses of 2, 10, or 50 μg RH5.1 formulated in AS01_B adjuvant at monthly intervals (2-2-2, red, n = 12; 10-10-10, blue, n = 27; 50-50-50,

(legend continued on next page)

mediated by a pool of purified IgG from RH5.1/AS01_B vaccinees. The same result was obtained when using the same concentration of RH5ΔNL protein. In contrast, no reversal of GIA was observed when using recombinant RH5-Nt, even at 8-fold higher molar concentration (Figure 1D). We also affinity-purified anti-RH5.1 and anti-RH5ΔNL human IgG, and both samples showed high-level growth inhibition. Following titration in the GIA assay, the RH5ΔNL-specific IgG showed a ~9-fold improvement in terms of the antigen-specific EC₅₀ (8 μg/mL, 95% confidence interval [CI]: 6–27), as compared to RH5.1-specific IgG (70 μg/mL, 95% CI: 50–114) (Figure 1E). These data show antibodies targeting the N terminus or intrinsic loop of RH5 do not contribute to functional GIA induced by the RH5.1 vaccine candidate. These data did not assess the small C terminus of RH5; however, we isolated a human IgG mAb, called R5.CT1, from an RH5.1/AS01_B vaccinee that recognized this region. The R5.CT1 clone specifically bound peptides 61 and 62 (Figure S1A) that together span the C-terminal 20 amino acids of RH5. Notably, mAb R5.CT1 showed no GIA against *P. falciparum* *in vitro* (Figure S1B). Together, these data suggest vaccine-induced human anti-RH5.1 IgG growth inhibitory antibodies recognize the alpha-helical core of the RH5 molecule and not the disordered regions. Also, the reason purified polyclonal RH5ΔNL-specific IgG is substantially more potent than RH5.1-specific IgG on a per μg basis is most likely due to the loss of these non-growth inhibitory responses.

RH5ΔNLC^{HS1}-SpyTag vaccine induces similar growth inhibitory antibodies to RH5ΔNL

In light of the aforementioned data and to initiate design of an improved RH5-based vaccine candidate, we first assessed three constructs based on the original design of the RH5ΔNL molecule. All three constructs were produced as soluble secreted proteins, using the Expres² *Drosophila* S2 stable cell line platform,³⁰ and purified by a C-terminal four amino acid C-tag³¹ — technologies that we previously used to biomanufacture the full-length RH5.1 protein for clinical trials.²⁰ Alongside the existing RH5ΔNL protein, we produced two additional molecules that also included the removal of the C-terminal 20 amino acids (to make “RH5ΔNLC”), followed by the addition of a C-terminal SpyTag (ST), prior to the C-tag, to enable conjugation to SpyCatcher (SC)-based display platforms.^{25,27} The first of these two molecules otherwise maintained the same RH5 sequence, which we termed “RH5ΔNLC-ST.” The second version, RH5ΔNLC^{HS1}-ST, used a previously reported RH5 sequence bearing 18 mutations, defined *in silico*, that confer improved molecular packing, surface polarity, and thermostability of the molecule without affecting its ligand binding or immunogenic proper-

ties³² (Figure 2A). Each protein was subsequently expressed from a polyclonal S2 stable cell line and purified from the supernatant by C-tag affinity and size-exclusion chromatography (SEC). Purified proteins ran at their expected molecular weights on an SDS-PAGE gel (Figure 2B). RH5ΔNLC-ST protein was also recognized by a panel of 14 human mAbs previously shown to span six distinct conformational epitope regions on the RH5 molecule³³ (Figure S2A). Notably, the RH5ΔNLC^{HS1}-ST protein showed greatly reduced or no mAb binding to one of these epitope sites and loss of binding of a single mAb at another site (Figure S2B), likely due to the introduction of the stabilizing mutations in this variant RH5 construct.³² Conversely, an approximately 8-fold higher yield on average of purified RH5ΔNLC^{HS1}-ST protein was achieved, as compared to RH5ΔNLC-ST and as anticipated when including the stabilizing mutations (Figure 2C).

To assess immunogenicity of the SpyTagged antigens, 2 μg each protein was formulated in Matrix-M adjuvant and used to immunize BALB/c mice intramuscularly three times at 3-week intervals. Anti-RH5 serum IgG responses were measured against full-length RH5.1 by ELISA after the first and final vaccinations. Following the first immunization, the RH5ΔNLC-ST protein was significantly more immunogenic than RH5ΔNL ($p = 0.02$, Dunn’s multiple comparison test); however, responses equalized for these two proteins after three immunizations. In contrast, RH5ΔNLC^{HS1}-ST showed significantly lower responses (~2- to 3-fold) after three doses as compared to RH5ΔNLC-ST (Figure 2D). This small reduction in recognition of the RH5.1 protein is likely explained by the introduction of the stabilizing mutations into the RH5ΔNLC^{HS1} construct. To determine if the stabilizing mutations in RH5ΔNLC^{HS1}-ST and/or C-terminal truncation in RH5ΔNLC would also affect the functional quality of the growth inhibitory antibody response, we purified the total IgG from pools of mouse sera (6 mice per antigen/group) and tested for *in vitro* GIA against *P. falciparum* (Figure 2E). Here, all three proteins could induce an anti-RH5 IgG response with very similar functional quality, i.e., same levels of GIA per unit of anti-RH5 IgG. Consequently, given (1) the comparable functional quality of anti-RH5 IgG induced by both SpyTagged proteins and (2) the very low production yield of RH5ΔNLC-ST, we elected to progress with the RH5ΔNLC^{HS1}-ST protein for further study despite the small reduction in overall immunogenicity and termed this construct “RH5.2-ST.”

Production of an RH5.2-HBsAg VLP

To produce a VLP-based vaccine candidate, we next tested conjugation of the RH5.2-ST protein to a HBsAg particle fused

green, $n = 9$) or a “delayed-fractional regimen” of two doses of 50 μg RH5.1 at 0 and 1 month and a third dose of 10 μg RH5.1 at 6 months (50-50-10, purple, $n = 12$). Individual responses are shown as measured 2–4 weeks post-third vaccination, with boxes indicating minimum, maximum, and median.

(C) Sera from volunteers receiving the 10-10-10 regimen of RH5.1/AS01_B ($n = 15$) were diluted 1:100 and tested against linear overlapping peptides spanning the RH5 vaccine insert, color-coded as per (A). Median, interquartile range (IQR), and range are shown for each peptide.

(D) Nine pooled total IgGs from the VAC063 study were tested by GIA with or without the indicated recombinant protein in two (RH5-Nt) or three (RH5.1 and RH5ΔNL) independent assays. The total IgGs were tested in a range from 3 to 9 mg/mL, at which each IgG showed ~60%–70% GIA on average (in the absence of protein). In each assay, the percentage of GIA reversal was calculated as $100 \times (1 - \frac{\text{percentage of GIA with protein}}{\text{percentage of GIA without protein}})$, and an average percentage of GIA reversal from two or three assays in individual IgGs (symbols) are shown with the median (bar) of the nine test IgGs.

(E) *In vitro* GIA of RH5.1-specific or RH5ΔNL-specific IgG affinity-purified from a pool of human sera collected 2 weeks post-final vaccination with RH5.1/AS01_B. The EC₅₀ (concentration of antigen-specific polyclonal IgG that gives 50% GIA, dashed line) was calculated by non-linear regression: RH5.1, $r^2 = 0.98$, $n = 19$; RH5ΔNL, $r^2 = 0.99$, $n = 20$.

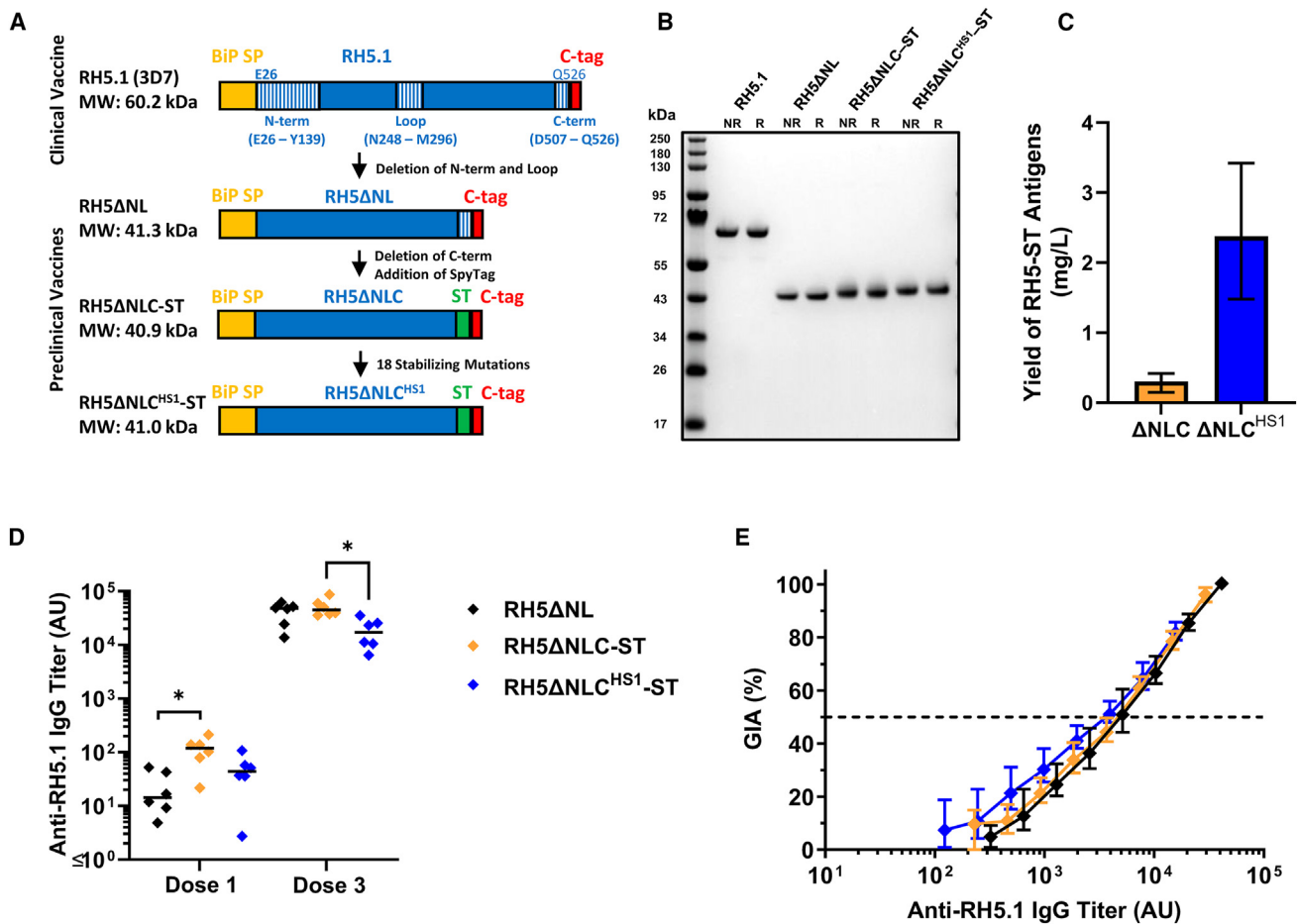


Figure 2. Expression and immunogenicity testing of SpyTagged-RH5ΔNLC constructs

(A) RH5 vaccine constructs based on *P. falciparum* 3D7 sequences. All have an N-terminal *Drosophila* BiP secretion signal peptide (SP; which is cleaved off during expression) and end with a C-terminal C-tag for affinity purification. Constructs with a SpyTag (ST) included a flexible (GSG)₃ linker preceding the ST to facilitate epitope accessibility once conjugated to a VLP bearing SpyCatcher. The predicted molecular weight (MW) of each construct based on the primary sequence and the relevant sequences of RH5 N terminus, loop, and C terminus are shown.

(B) Non-reduced (NR) and reduced (R) SDS-PAGE gel of affinity and SEC-purified RH5.1, RH5ΔNL, RH5ΔNLC-ST, and RH5ΔNLC^{HS1}-ST proteins.

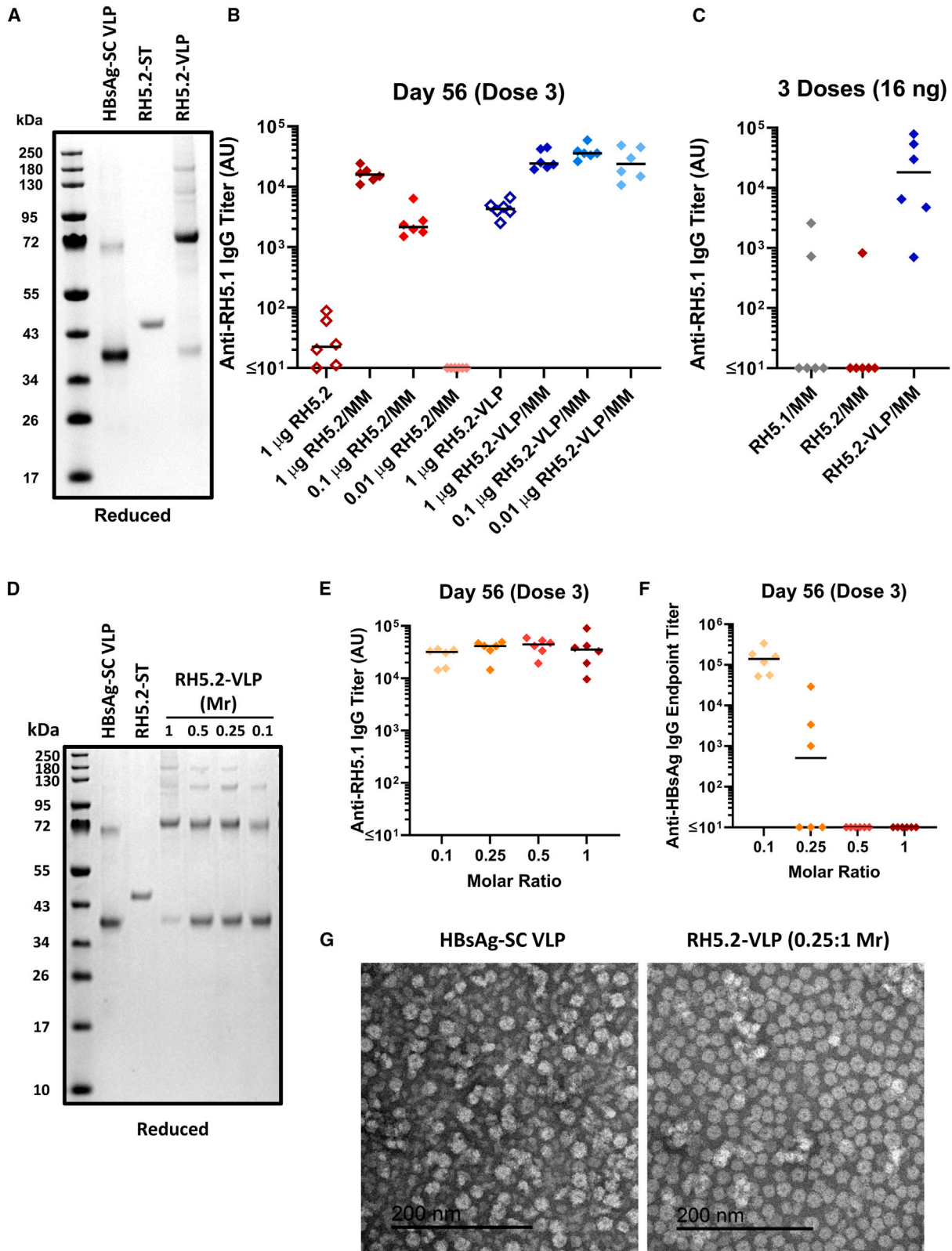
(C) Final yield of RH5 protein (in mg) purified from 1 L of *Drosophila* S2 stable cell line supernatant. Bars show the mean yield and error bars the range from n = 3 independent purification campaigns for each protein.

(D) BALB/c mice (n = 6 per group) were immunized intramuscularly with three 2 μg doses (on days 0, 21, and 42) of RH5ΔNL, RH5ΔNLC-ST, or RH5ΔNLC^{HS1}-ST, all formulated in Matrix-M adjuvant. Anti-RH5 (full-length RH5.1) IgG titers were measured in the serum by ELISA after dose 1 (day 20) and dose 3 (day 70). Each point represents a single mouse and the line represents the median. Analyses using Kruskal-Wallis test with Dunn's multiple comparison test across the three groups at each time point; *p < 0.05.

(E) A single-cycle *in vitro* GIA assay against 3D7 clone *P. falciparum* parasites was performed with total purified IgG from pooled mouse sera (n = 6 mice pooled per group). GIA is plotted against the anti-RH5 (full-length RH5.1) titer measured by ELISA in each purified total IgG to assess functional antibody quality, i.e., GIA per unit anti-RH5.1 IgG. Data show titration curve for each sample, with points showing the mean and range of n = 3 replicates per test condition.

to SC (HBsAg-SC).²⁷ We initially conjugated the RH5.2-ST to HBsAg-SC in a 1:1 M ratio. Following an overnight conjugation reaction, any free unconjugated RH5.2-ST protein was removed by SEC, thereby leaving the conjugated RH5.2-HBsAg VLP product. Analysis by reducing SDS-PAGE showed the expected banding pattern for HBsAg-SC with a dominant monomer band (~37.0 kDa) as well as multimers (Figure 3A). Following conjugation, a new band corresponding to the RH5.2-HBsAg monomer unit was observed at the expected size of ~77 kDa along with other bands corresponding to the expected multimers at higher

molecular weight. Free unconjugated RH5.2-ST protein was not observed following its removal by SEC, although some unconjugated HBsAg-SC monomer units remained within the VLP preparation. Analysis by densitometry indicated a conjugation efficiency of ~80%. A study in BALB/c mice was performed next to compare the immunogenicity of RH5.2-ST-soluble protein versus the RH5.2-VLP. Dosing of the RH5.2-VLP was adjusted in each case to deliver the same molar amount of RH5.2 antigen as the soluble protein comparator (Figure 3B). Following three immunizations, the RH5.2-VLP formulated in Matrix-M adjuvant



(legend on next page)

showed comparable anti-RH5 serum IgG responses across all three doses tested (1, 0.1, and 0.01 μg ; $p = 0.39$, Kruskal-Wallis test). In contrast, the same analysis with soluble RH5.2-ST protein showed a clear dose response, with no antibodies detected at the lowest 0.01 μg dose ($p < 0.0001$, Kruskal-Wallis test). When comparing across the same doses of soluble RH5.2-ST versus the RH5.2-VLP, only the 1 μg dose showed comparable immunogenicity, while the RH5.2-VLP was significantly more immunogenic at the lower doses ($p = 0.002$ for both the 0.1 and 0.01 μg doses, Dunn's multiple comparison test). Finally, in the absence of adjuvant, a 1 μg dose of the RH5.2-VLP still induced responses, albeit at a lower level than when using Matrix-M adjuvant; in contrast, the soluble protein showed negligible immunogenicity (Figure 3B). Analysis of responses following the first and second vaccinations also showed that the 1 and 0.1 μg doses of RH5.2-VLP formulated in Matrix-M primed detectable serum antibody responses after only a single immunization and achieved maximal titers after two immunizations. In all cases, the RH5.2-VLP was more immunogenic than the soluble protein (Figures S3A and S3B). A second experiment was performed using the same total dose of antigen to mirror clinical practice; here, given that a maximum dose of 50 μg of RH5.1 has been tested in adult humans^{21,22} (with an assumed average body weight of ~ 70 kg), we adjusted the dose to 16 ng for mice (average body weight of ~ 22 g). Hence, a 16 ng total protein dose of the RH5.2-VLP was compared to a 16 ng dose of soluble RH5.2-ST or soluble RH5.1 (the current lead clinical antigen); all were formulated in Matrix-M adjuvant. Following three immunizations, only the RH5.2-VLP showed high-titer anti-RH5 serum IgG responses in contrast to negligible immunogenicity observed with either soluble protein vaccine (Figure 3C). Both experiments confirmed the RH5.2-VLP is inherently more immunogenic than soluble RH5 protein in mice.

However, despite the highly promising immunogenicity, ongoing studies indicated the conjugated RH5.2-VLP was prone to precipitation during production, resulting in substantial loss of product. We thus attempted to optimize reaction conditions by increasing the salt concentration and lowering the temperature, as well as by combining the two components (RH5.2-ST and HBsAg-SC) dropwise. We also tested incubation of the two com-

ponents in different molar ratios (RH5.2-ST:HBsAg-SC as 1:1, 0.5:1, 0.25:1, and 0.1:1); here, as expected, more unconjugated HBsAg-SC monomer units remained when combining the VLP with less RH5.2-ST (Figure 3D). Precipitation was also greatly decreased, and overall process yield increased when using the 0.25:1 or 0.1:1 M ratios in the conjugation reaction. We therefore next proceeded to screen the different products for immunogenicity. BALB/c mice were immunized three times with the four different RH5.2-VLPs all formulated in Matrix-M adjuvant. Dosing was adjusted in each case to deliver the same molar amount of RH5.2 antigen (10 ng). Interestingly, maximal titers were reached faster with VLPs produced using the lower molar ratios (Figures S4A and S4B), although following three doses all preparations showed comparable anti-RH5.1 serum IgG responses (Figure 3E). Serum antibody responses against the HBsAg VLP carrier inversely related to the molar ratio used in the conjugation reaction, with no detectable responses in mice immunized with the RH5.2-VLP produced using the 1:1 or 0.5:1 ratio (Figure 3F). These higher anti-HBsAg responses, especially in the 0.1:1 M ratio group, could have been due to the higher total protein dose used in this experiment and/or excess of unconjugated HBsAg-SC subunits on these particles. Nevertheless, we proceeded with further study and evaluation of the RH5.2-VLP produced using the 0.25:1 ratio, as a balanced trade-off with regard to production yield versus strong anti-RH5.2 immunogenicity and low anti-HBsAg VLP carrier immunogenicity. Further analysis of this product by transmission electron microscopy confirmed particles of the expected ~ 20 nm in size (Figure 3G). The RH5.2-VLP was also recognized by the same anti-RH5 human mAbs as reacted with the parental RH5 Δ NLC^{HS1}-ST protein, confirming the presence and accessibility of these critical conformational epitopes on the VLP (Figure S2C).

The growth inhibitory antibody response induced by the RH5.2-VLP is superior to RH5.1

In a final study, we compared the functional immunogenicity of the RH5.2-VLP to soluble RH5.2-ST protein and the current clinical antigen (soluble RH5.1 protein) in Wistar rats. All antigens were formulated in Matrix-M adjuvant and administered

Figure 3. Production and immunogenicity testing of the RH5.2-VLP vaccine candidate

- (A) Reducing SDS-PAGE gel of HBsAg-SC VLP and RH5.2-ST protein. These proteins were conjugated together in a 1:1 M ratio. The resulting RH5.2-VLP was SEC purified and is run in the final lane.
- (B) BALB/c mice ($n = 6$ per group) were immunized intramuscularly with three doses of RH5.2-ST protein ("RH5.2"), or RH5.2-VLP on days 0, 21, and 42 either with (closed symbols) or without (open symbols) Matrix-M (MM) adjuvant. Dosing of the RH5.2-VLP was adjusted in each case to deliver the same molar amount of RH5.2 antigen as the soluble protein comparator (1, 0.1, or 0.01 μg). Anti-RH5 (full-length RH5.1) IgG titers were measured in the serum by ELISA after three doses at day 56. Each point represents a single mouse and the line represents the median.
- (C) BALB/c mice ($n = 6$ per group) were immunized intramuscularly with three doses of RH5.1 protein, RH5.2-ST protein ("RH5.2"), or RH5.2-VLP on days 0, 21, and 42. All vaccines used a total dose of 16 ng formulated in MM adjuvant. Anti-RH5 (full-length RH5.1) IgG titers were measured in the serum by ELISA after three doses at day 56. Each point represents a single mouse and the line represents the median.
- (D) Reducing SDS-PAGE gel as in (A) but showing RH5.2-VLP produced by conjugating RH5.2-ST and HBsAg-SC VLP components at the indicated molar ratios (Mr).
- (E) BALB/c mice ($n = 6$ per group) were immunized intramuscularly with three doses of RH5.2-VLP, produced using the indicated Mr of RH5.2-ST to HBsAg-SC (0.1:1, 0.25:1, 0.5:1, and 1:1), on days 0, 21, and 42. Dosing was adjusted in each case to deliver the same molar amount of RH5.2 antigen (10 ng); total RH5.2-VLP dose = 232, 52, 40, and 23 ng, respectively. All vaccines were formulated in MM adjuvant. Anti-RH5 (full-length RH5.1) IgG titers and (F) anti-HBsAg IgG titers were measured in the serum by ELISA after three doses at day 56. Each point represents a single mouse and the line represents the median.
- (G) Negatively stained transmission electron microscopy (TEM) image of HBsAg-SC VLP starting material and RH5.2-VLP vaccine made using the 0.25:1 Mr. Scale bar 200 nm.

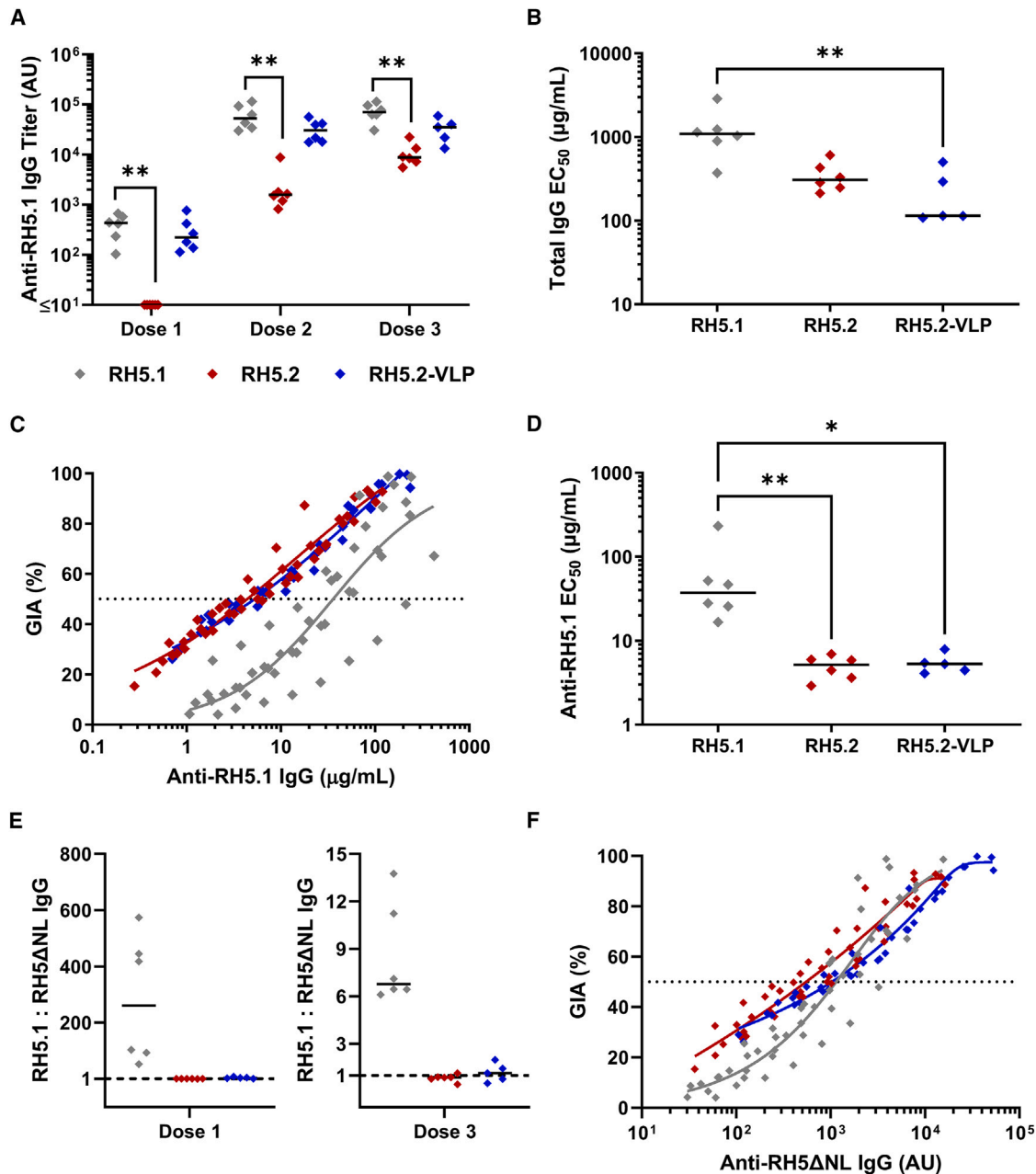


Figure 4. Functional immunogenicity testing of RH5.1, RH5.2, and the RH5.2-VLP in rats

(A) Wistar rats ($n = 6$ per group) were immunized intramuscularly with three doses of RH5.1 protein, RH5.2-ST (“RH5.2”) protein, or RH5.2-VLP on days 0, 28, and 56. All vaccines used a total dose of $2 \mu\text{g}$ formulated in MM adjuvant. Anti-RH5 (full-length RH5.1) IgG titers were measured in the serum by ELISA after each dose on days 14, 42, and 70, respectively, for doses 1–3. Each point represents a single rat and the line the median; $n = 5$ for dose 3 of RH5.2-VLP as a single rat was euthanized after a problem with a study-related procedure. Analysis using Kruskal-Wallis test with Dunn’s multiple comparison test across the three vaccine groups with each dose result analyzed separately; $**p < 0.01$.

(B) A single-cycle *in vitro* GIA assay against 3D7 clone *P. falciparum* parasites was performed with total IgG purified from serum from each vaccinated rat post-final immunization ($n = 5$ –6 per group). Total IgG was titrated in the assay, and the concentration in mg/mL required to achieve 50% GIA (EC_{50}) was interpolated. Data show the EC_{50} for each rat and the line shows the median. Analysis using Kruskal-Wallis test with Dunn’s multiple comparison test; $**p < 0.01$.

(C) GIA data plotted against the anti-RH5.1 IgG concentration measured by quantitative ELISA in each purified total IgG to assess functional antibody quality, i.e., GIA per μg anti-RH5.1 IgG. A non-linear regression curve is shown for all samples combined in each vaccine group (RH5.1: $r^2 = 0.75$, $n = 144$; RH5.2: $r^2 = 0.93$, $n = 143$; RH5.2-VLP: $r^2 = 0.96$, $n = 120$). The dashed line indicates 50% GIA.

(D) The concentration of RH5.1-specific IgG in $\mu\text{g/mL}$ required to achieve 50% GIA (EC_{50}) was interpolated by non-linear regression for each individual rat from the data in (C). Data show the EC_{50} for each rat and the line shows the median. Analysis using Kruskal-Wallis test with Dunn’s multiple comparison test; $*p < 0.05$, $**p < 0.01$.

(legend continued on next page)

intramuscularly. Groups of six animals were immunized three times, at monthly intervals, using the same total dose of vaccine (2 μ g) to mirror clinical practice. Serum IgG antibody levels were assessed against full-length RH5.1 by ELISA. Responses induced by RH5.1 and the RH5.2-VLP reached maximal levels after two doses and were superior to soluble RH5.2-ST after every vaccine dose, with RH5.1 significant versus RH5.2-ST (Figure 4A). Following the third dose, total IgG was purified from serum and titrated in the assay of GIA against *P. falciparum* parasites. Here, the RH5.2-VLP showed significantly improved GIA over RH5.1, with the median EC₅₀ of total IgG 9.6-fold lower (Figure 4B). Given the comparable quantitative immunogenicity shown by RH5.1 and the RH5.2-VLP (Figure 4A), we next assessed the functional quality of the RH5.1-specific IgG by plotting the GIA data versus ELISA performed on the purified total IgG (Figure 4C). Here, the antibodies induced in the RH5.2-VLP and RH5.2-ST protein-immunized groups showed identical quality, i.e., the same GIA per μ g of RH5.1-specific IgG, and both significantly improved upon the functional quality induced by RH5.1 immunization (Figure 4D). These data suggest the functional quality of RH5.2-induced IgG is comparable with soluble protein or VLP delivery. Consequently, the improvement in overall levels of GIA observed with the RH5.2-VLP (Figure 4B) relate to its superior quantitative immunogenicity (when comparing to soluble RH5.2) and superior qualitative immunogenicity (when comparing to RH5.1). Given our earlier data indicated the N terminus and intrinsic loop of RH5 do not contribute to functional GIA induced by RH5.1 in humans, we hypothesized the improvement in functional antibody quality seen with RH5.2 over RH5.1 in the rats was due to loss of responses against these disordered regions of the molecule. We thus tested the rat sera by ELISA against RH5 Δ NL and compared the ratio of this response to the RH5.1 response (Figure 4E). As expected, the ratios for RH5.2 and RH5.2-VLP were approximately one, given the RH5.2 immunogen is based on the RH5 Δ NL structure, and thus ELISA with either RH5.1 or RH5 Δ NL should give a comparable readout. However, the ratio of RH5.1:RH5 Δ NL-specific IgG induced by the RH5.1 vaccine was \sim 250 following the first dose, suggesting the RH5 Δ NL antibody response is initially sub-dominant to responses against the N terminus and intrinsic loop present in RH5.1. This sub-dominance decreases after three vaccine doses, with the ratio reduced to \sim 6.5 (Figure 4E). Overall, these ELISA data suggested a substantial antibody response is mounted to the N terminus and/or intrinsic loop when using RH5.1. To explore this further, we also conducted a second quality analysis by re-plotting the GIA data versus ELISA on the purified IgG performed against RH5 Δ NL protein. Here, in support of our hypothesis, all three constructs now performed similarly, with each on average achieving 50% GIA at approximately the same level of anti-RH5 Δ NL IgG (Figure 4F). These data strongly suggest all of the GIA induced in the rats

by RH5.1 was mediated by the subset of IgG that recognizes RH5 Δ NL, in agreement with the observations in human vaccine responses (Figure 1).

DISCUSSION

The development of a highly effective vaccine against the pathogenic blood-stage infection of human malaria will require a delivery platform that can induce an antibody response of both maximal quantity and functional quality. One strategy to achieve this includes presenting antigens to the immune system on VLPs. To select a vaccine antigen design, we first explored functional responses induced in UK adults vaccinated with RH5.1/AS01_B.²¹ These analyses indicated that antibodies raised to the three disordered regions of the RH5_FL do not make a measurable contribution to the overall levels of GIA. These data are consistent with previous reports showing that murine or human mAbs targeting the N terminus or intrinsic loop do not inhibit *P. falciparum* growth *in vitro*^{33,34} and that high-dose passive transfer of a mAb against the intrinsic loop failed to protect *Aotus* monkeys against *P. falciparum* challenge.²³ In contrast to the results reported here, another study reported that RH5-Nt binds the parasite protein P113 and that vaccination of rabbits with RH5-Nt protein could induce antibodies that mediate modest levels of GIA³⁵; however, we could not identify a similar contribution of anti-RH5-Nt IgG to the GIA induced by human RH5.1 vaccination in our studies. Our data are also consistent with other studies that have since questioned the significance of P113 in merozoite invasion. In particular, one study found anti-P113 antibodies that block the interaction with RH5-Nt are GIA negative,³⁶ while another reported P113 plays an important role in maintaining normal architecture of the parasitophorous vacuole membrane within the infected erythrocyte.³⁷ Moreover, it has since been reported that RH5-Nt is cleaved off the RH5 molecule within the micronemes of the *P. falciparum* parasite by the aspartic protease plasmepsin X prior to release of RH5 to the merozoite surface,³⁸ suggesting it would be an unlikely target of antibodies. In summary, these data strongly suggest these regions of disorder within RH5_FL are not targets of functional IgG. This conclusion is further supported by our data showing the RH5 Δ NL protein could reverse all GIA induced by human RH5.1 vaccination, suggesting that all growth inhibitory epitopes targeted by the human IgG are located within this protein construct; this is also consistent with known epitope information of anti-RH5 murine and human mAbs reported previously and shown to have anti-parasitic activity.^{29,33,34,39} Finally, our data showed a \sim 9-fold improvement in the antigen-specific GIA EC₅₀ potency when comparing affinity-purified polyclonal IgG specific for RH5 Δ NL versus RH5.1. We thus elected to focus vaccine design efforts on a molecule lacking all three disordered regions, which we termed “RH5 Δ NLC.”

(E) Ratio of the serum IgG ELISA response as measured using the RH5.1 and RH5 Δ NL proteins after the first and third vaccinations. Data shown for each rat (n = 5–6 per group) and the line shows the median.

(F) GIA data plotted against the anti-RH5 Δ NL IgG titer measured by ELISA with AU readout in each purified total IgG to assess functional antibody quality, i.e., GIA per unit anti-RH5 Δ NL IgG. A non-linear regression curve is shown for all samples combined in each vaccine group (RH5.1: $r^2 = 0.86$, n = 144; RH5.2: $r^2 = 0.90$, n = 143; RH5.2-VLP: $r^2 = 0.95$, n = 120). The dashed line indicates 50% GIA.

To prepare for the biomanufacture of clinical-grade immunogen, we produced protein constructs utilizing the same expression and purification platform technologies as those used previously for the clinical biomanufacture of RH5.1.²⁰ Consistent with the original report,³² the yield of purified SpyTagged RH5 Δ NLC protein was \sim 8-fold higher when incorporating the stabilizing mutations. Immunization of mice with these monomeric soluble proteins-in-adjuvant showed a modestly higher antibody response, as measured against RH5.1 antigen, when using the wild-type sequence proteins as compared to the mutated version. Consistent with this, we noted reduced binding or loss of binding by human mAbs at two previously identified antigenic sites within the RH5 Δ NLC molecule,³³ indicating that a small number of specific antibody epitopes were affected by the stabilizing mutations. However, regardless of this and consistent with the original report of the stabilized RH5 Δ NLC sequence,³² we observed no difference in the functional quality of the RH5-specific antibodies elicited through vaccination of mice with these SpyTagged proteins formulated in Matrix-M adjuvant. Whether these mutations would significantly impact immune responses in humans remains to be determined. Given the substantially higher yield of the stabilized RH5 Δ NLC SpyTagged variant, we proceeded with this stabilized version of the RH5 Δ NLC protein, which we termed “RH5.2-ST.”

VLP-based immunogens, that deliver multimeric or arrayed antigen, have been widely shown to offer numerous advantages over soluble antigen vaccines. These include improved trafficking to draining lymph nodes, improved efficiency of B cell receptor cross-linking, as well as oriented antigen display, all of which can substantially improve quantitative and/or qualitative antibody immunogenicity.^{40,41} Here, we used HBsAg, which forms lipoprotein VLPs, \sim 20–30 nm in size with \sim 100 monomeric subunits.⁴² Our initial attempts to conjugate RH5.2-ST to HBsAg-SC VLPs at a 1:1 M ratio showed a maximal conjugation efficiency of \sim 80% by densitometry analysis; however, the overall process yield was very low due to significant precipitation and loss of product during the conjugation process. Reaction conditions were optimized leading to improved yield, but this necessitated conjugating RH5.2-ST at a lower molar ratio, with 0.25:1 enabling sufficient yield. Possible disadvantages to the presence of excess unconjugated HBsAg subunits within the VLPs are that lower amounts of RH5.2 antigen are administered per μ g total vaccine; however, our immunogenicity data in mice suggested this was not a problem, consistent with other reports using the same vaccine delivery platform with the Pfs25 malaria antigen.²⁷ It is also possible that pre-existing anti-HBsAg antibody responses may impact the vaccine antigen-specific responses; however, other preclinical data in mice suggest this is not the case.²⁷ Moreover, analysis of RTS,S/AS01 immunogenicity in humans (another recombinant vaccine which comprises chimeric HBsAg VLPs and which could only be manufactured when \sim 20% of subunits were fused to CSP⁴³) also suggests similar, with no correlation observed between baseline anti-HBsAg antibodies and anti-CSP vaccine immunogenicity after 3 doses.⁴⁴ Nonetheless, efforts to re-design RH5-based protein immunogens with improved solubility characteristics currently remain the focus of ongoing work.

We subsequently undertook a series of mouse immunogenicity studies comparing the RH5.2-VLP versus the soluble RH5.2 and RH5.1 vaccine candidates. Notably, quantitative antibody immunogenicity in mice was determined by the presence of adjuvant, the number of immunizations, and the immunogen dose. These data showed the RH5.2-VLP was consistently more immunogenic than soluble antigen after three immunizations and when tested (1) at low dose (in the 10–100 ng range) in the presence of Matrix-M adjuvant and (2) at high dose (1 μ g) in the absence of Matrix-M adjuvant. Responses induced by the RH5.2-VLP in Matrix-M adjuvant were also higher after one or two immunizations and reached maximal titers earlier, across the dose range tested, as compared to soluble antigen. Moreover, similar to a previous study of the transmission-blocking malaria antigen Pfs25 conjugated to HBsAg VLPs,²⁷ maximal anti-RH5 serum IgG responses were achieved following three immunizations of the RH5.2-VLP in Matrix-M adjuvant, regardless of RH5.2 conjugation density to the HBsAg VLP.

We subsequently proceeded to further test the RH5.2-VLP produced using the 0.25:1 M ratio in rats. Here, the RH5.2-VLP showed improvement over RH5.1, driven by a significantly lower antigen-specific EC₅₀ of the vaccine-induced IgG, with RH5.2-vaccinated rats achieving 50% GIA at median levels of \sim 5 μ g/mL RH5.1-specific antibody. Notably, this qualitative improvement was consistent across all RH5.2-vaccinated rats, whether immunized with soluble antigen or the HBsAg-VLP. This indicates no added benefit of VLP delivery with regard to qualitative immunogenicity and that the conjugated RH5.2 is likely fully exposed and/or flexibly displayed on the VLP surface. Consistent with this, the mAb panel analysis detected the identical range of epitopes on both soluble and VLP-conjugated RH5.2 antigen, including those in the C-terminal region of RH5.2^{33,45} that would be expected to be closer to the VLP surface. In summary, vaccination with the RH5.2 immunogen, itself based on the RH5 Δ NLC molecule, induced a serum antibody response in rats of superior functional quality per unit of anti-RH5.1 IgG as compared to the current clinical lead vaccine RH5.1/Matrix-M. This improvement was most likely due to the loss of non-functional IgG responses against the disordered regions of the RH5_FL (when using RH5.2), which appear to dilute the subdominant and functional IgG induced against the helical core (when using RH5.1). In parallel, VLP-based delivery improved quantitative immunogenicity against the smaller RH5.2 immunogen, thereby leading to the highest levels of GIA observed in rats with the RH5.2-VLP. It will now be important to establish in humans whether the RH5.2-VLP/Matrix-M vaccine candidate can induce comparable improvements in antibody quantity and/or quality to those observed in mice or rats, thereby leading to an improvement in protection against blood-stage *P. falciparum*. Indeed, the RH5.2-VLP antigen has since completed biomanufacturing in line with current good manufacturing practice and has entered phase 1a/b clinical trials in the United Kingdom and The Gambia ([ClinicalTrials.gov](https://clinicaltrials.gov/ct2/show/study/NCT05978037) NCT05978037 and NCT05357560) formulated with Matrix-M adjuvant. These will enable the comparison in humans of the RH5-based immunogens delivered as a soluble protein versus an array on HBsAg-VLPs.

Limitations of this study

Firstly, due to human sample limitations, some experiments necessitated the use of pooled sera, and we could not draw conclusions about responses at the individual level. Secondly, all vaccines were recombinant and were only tested in rodent models using a single adjuvant. It remains possible that other adjuvants and/or vaccine delivery platforms (such as mRNA) could show different results, and these warrant future investigation. It is also currently unknown whether our preclinical observations in mice and rats will translate to larger species; however, assessment of the RH5.2-VLP/Matrix-M vaccine candidate in ongoing phase 1a/b clinical trials will provide valuable data to address this.

STAR★METHODS

Detailed methods are provided in the online version of this paper and include the following:

- [KEY RESOURCES TABLE](#)
- [RESOURCES AVAILABILITY](#)
 - Lead contact
 - Materials availability
 - Data and code availability
- [EXPERIMENTAL MODEL AND SUBJECT DETAILS](#)
 - VAC063 clinical trial samples
 - Mice
 - Rats
 - Cell lines
- [METHOD DETAILS](#)
 - Model of RH5.1
 - Generation of polyclonal Schneider 2 (S2) stable cell lines
 - Expression and purification of recombinant RH5 proteins
 - SDS-PAGE
 - Production of anti-RH5 monoclonal antibodies
 - Conjugation of RH5.2-ST to HBsAg-SC VLPs
 - Negative staining transmission electron microscopy (TEM)
 - Rodent immunization studies
 - Monoclonal antibodies
 - Monoclonal antibody ELISA
 - Standardized ELISAs
 - RH5 peptide ELISAs
 - Anti-HBsAg endpoint ELISA
 - Assay of growth inhibition activity (GIA)
- [QUANTIFICATION AND STATISTICAL ANALYSIS](#)
- [ADDITIONAL RESOURCES](#)

SUPPLEMENTAL INFORMATION

Supplemental information can be found online at <https://doi.org/10.1016/j.xcrm.2024.101654>.

ACKNOWLEDGMENTS

The authors are grateful for the assistance of Julie Furze, Penelope Lane, Fay Nugent, Wendy Crocker, Charlotte Hague, Daniel Alanine, Robert Ragothe, Darren Leneghan, Geneviève Labbé, Carolyn Nielsen, Martino Bardelli, Jenny Bryant, Lana Strmecki, and Matt Higgins (University of Oxford); Sally Pelling-Deeves for arranging contracts (University of Oxford); Colleen Woods (PATH-MVI); Jenny Reimer (Novavax); Ken Tucker, Timothy Phares, Jayne Christen, Cecille Browne, and Vin Kotraiah (Leidos); Robin Miller (USAID); and all the VAC063 trial participants.

This work was funded in part by the UK Medical Research Council (MR/P01351/1)—this UK funded award was part of the EDCTP2 programme supported by the European Union; the European Union's Horizon 2020 research

and innovation programme under a grant agreement for OptiMalVax (733273); the PATH Malaria Vaccine Initiative; the UK MRC Confidence in Concept (CiC) Tropical Infectious Disease Consortium (MC_PC_15040); and the Wellcome Trust through a Translation Award (205981/Z/17/Z). This work, as well as the VAC063 clinical trial, was made possible in part through support provided by the Infectious Disease Division, Bureau for Global Health, United States Agency for International Development (USAID), under the terms of the Malaria Vaccine Development Program (MVDP) (AID-OAA-C-15-00071), for which Leidos Inc. was the prime contractor, and under the terms of GH-BAA-2018-Addendum03 (7200AA20C00017), for which PATH is the prime contractor. The GIA assays were supported in part by the Division of Intramural Research of the National Institute of Allergy and Infectious Diseases, National Institutes of Health, and by an Interagency Agreement (AID-GH-T-15-00001) between the USAID MVDP and NIAID, NIH. The findings and conclusions are those of the authors and do not necessarily represent the official position of USAID. This work was also supported in part by the National Institute for Health Research Oxford Biomedical Research Centre (BRC), NHS Blood and Transplant (NHSBT; who provided material), and Wellcome Trust, UK; the views expressed are those of the authors and not necessarily those of the NIHR or the Department of Health and Social Care or NHSBT. GSK had the opportunity to review the manuscript but content is the sole responsibility of the authors. J.S. held a Wellcome/African Academy of Sciences DELTAS Africa Grant Master's Studentship (DEL-15-007: Awandare). B.G.W. held a UK MRC PhD Studentship (MR/N013468/1). S.B. and S.J.D. are Jenner Investigators and S.J.D. held a Wellcome Trust Senior Fellowship (106917/Z/15/Z).

For the purpose of Open Access, the author has applied a CC BY public copyright license to any Author Accepted Manuscript (AAM) version arising from this submission.

AUTHOR CONTRIBUTIONS

Conceived and performed experiments and/or analyzed the data, L.D.W.K., D.P., J.R.B., H.D., D.Q., A.M.L., S.E.S., D.J.P., A.D., B.G.W., K. McHugh, A.R., C.A.R., V.S., J.S., C.R.-S., R.A.D., A.S.I., Y.Z., G.G., J.J., Y.L., K. Miura, and S.J.D.; performed project management, A.R.N., R.S.M., C.R.K., A.J.B., L.A.S., R.A., and K.S.; contributed reagents, materials, and analysis tools, C.C., A.M.M., I.C., S.J.F., C.A.L., M.R.H., and S.B.; wrote the paper, L.D.W.K. and S.J.D.

DECLARATION OF INTERESTS

S.J.D. is an inventor on patent applications relating to RH5 malaria vaccines and antibodies, is a co-founder of and shareholder in SpyBiotech, and has been a consultant to GSK on malaria vaccines.

A.M.M. has been a consultant to GSK on malaria vaccines, has an immediate family member who is an inventor on patent applications relating to RH5 malaria vaccines and antibodies, and is a co-founder of and shareholder in SpyBiotech.

M.R.H. is an inventor on patents relating to peptide targeting via spontaneous amide bond formation and is a co-founder of and shareholder in SpyBiotech.

S.B. is an inventor on patent applications relating to vaccines made using spontaneous amide bond formation and is a co-founder of, shareholder in, and employee of SpyBiotech.

J.J. is an inventor on patent applications relating to vaccines made using spontaneous amide bond formation and is a co-founder of and shareholder in SpyBiotech.

R.A.D. is an inventor on patent applications relating to vaccines made using spontaneous amide bond formation and shareholder in SpyBiotech.

L.D.W.K., J.R.B., D.Q., A.M.L., S.E.S., B.G.W., K. McHugh, I.C., S.J.F., and D.P. are inventors on patent applications relating to RH5 malaria vaccines and/or antibodies.

Received: January 5, 2024

Revised: April 12, 2024

Accepted: June 19, 2024

Published: July 16, 2024

REFERENCES

- World Health Organization (2023). World Malaria Report, <https://www.who.int/teams/global-malaria-programme/reports/world-malaria-report-2023>.
- Rts, S.C.T.P. (2015). Efficacy and safety of RTS,S/AS01 malaria vaccine with or without a booster dose in infants and children in Africa: final results of a phase 3, individually randomised, controlled trial. *Lancet* 386, 31–45.
- Datoo, M.S., Dicko, A., Tinto, H., Ouédraogo, J.B., Hamaluba, M., Olotu, A., Beaumont, E., Ramos Lopez, F., Natama, H.M., Weston, S., et al. (2024). Safety and efficacy of malaria vaccine candidate R21/Matrix-M in African children: a multicentre, double-blind, randomised, phase 3 trial. *Lancet* 403, 533–544.
- Dicko, A., Ouedraogo, J.B., Zongo, I., Sagara, I., Cairns, M., Yerbanga, R.S., Issiaka, D., Zoungrana, C., Sidibe, Y., Tapily, A., et al. (2023). Seasonal vaccination with RTS,S/AS01(E) vaccine with or without seasonal malaria chemoprevention in children up to the age of 5 years in Burkina Faso and Mali: a double-blind, randomised, controlled, phase 3 trial. *Lancet Infect. Dis.* 24, 75–86.
- Chandramohan, D., Zongo, I., Sagara, I., Cairns, M., Yerbanga, R.S., Diarra, M., Nikiéma, F., Tapily, A., Sompougdou, F., Issiaka, D., et al. (2021). Seasonal Malaria Vaccination with or without Seasonal Malaria Chemoprevention. *N. Engl. J. Med.* 385, 1005–1017.
- Meremikwu, M.M., Donegan, S., Sinclair, D., Esu, E., and Oringanje, C. (2012). Intermittent preventive treatment for malaria in children living in areas with seasonal transmission. *Cochrane Database Syst. Rev.* 2012, CD003756.
- Topazian, H.M., Schmit, N., Gerard-Ursin, I., Charles, G.D., Thompson, H., Ghani, A.C., and Winskill, P. (2023). Modelling the relative cost-effectiveness of the RTS,S/AS01 malaria vaccine compared to investment in vector control or chemoprophylaxis. *Vaccine* 41, 3215–3223.
- Draper, S.J., Sack, B.K., King, C.R., Nielsen, C.M., Rayner, J.C., Higgins, M.K., Long, C.A., and Seder, R.A. (2018). Malaria Vaccines: Recent Advances and New Horizons. *Cell Host Microbe* 24, 43–56.
- Wright, G.J., and Rayner, J.C. (2014). Plasmodium falciparum erythrocyte invasion: combining function with immune evasion. *PLoS Pathog.* 10, e1003943.
- Douglas, A.D., Williams, A.R., Illingworth, J.J., Kamuyu, G., Biswas, S., Goodman, A.L., Wyllie, D.H., Crosnier, C., Miura, K., Wright, G.J., et al. (2011). The blood-stage malaria antigen PFRH5 is susceptible to vaccine-inducible cross-strain neutralizing antibody. *Nat. Commun.* 2, 601.
- Ragotte, R.J., Higgins, M.K., and Draper, S.J. (2020). The RH5-CyRPA-Ripr Complex as a Malaria Vaccine Target. *Trends Parasitol.* 36, 545–559.
- Scally, S.W., Triglia, T., Evelyn, C., Seager, B.A., Pasternak, M., Lim, P.S., Healer, J., Geoghegan, N.D., Adair, A., Tham, W.H., et al. (2022). PCR complex is essential for invasion of human erythrocytes by Plasmodium falciparum. *Nat. Microbiol.* 7, 2039–2053.
- Farrell, B., Alam, N., Hart, M.N., Jamwal, A., Ragotte, R.J., Walters-Morgan, H., Draper, S.J., Knuepfer, E., and Higgins, M.K. (2023). The PFR complex bridges malaria parasite and erythrocyte during invasion. *Nature* 625, 578–584.
- Crosnier, C., Bustamante, L.Y., Bartholdson, S.J., Bei, A.K., Theron, M., Uchikawa, M., Mboup, S., Ndir, O., Kwiatkowski, D.P., Duraisingh, M.T., et al. (2011). Basigin is a receptor essential for erythrocyte invasion by Plasmodium falciparum. *Nature* 480, 534–537.
- Volz, J.C., Yap, A., Sisquella, X., Thompson, J.K., Lim, N.T.Y., Whitehead, L.W., Chen, L., Lampe, M., Tham, W.H., Wilson, D., et al. (2016). Essential Role of the PFRh5/PfRipr/CyRPA Complex during Plasmodium falciparum Invasion of Erythrocytes. *Cell Host Microbe* 20, 60–71.
- Galaway, F., Yu, R., Constantinou, A., Prugnolle, F., and Wright, G.J. (2019). Resurrection of the ancestral RH5 invasion ligand provides a molecular explanation for the origin of P. falciparum malaria in humans. *PLoS Biol.* 17, e3000490.
- Douglas, A.D., Baldeviano, G.C., Lucas, C.M., Lugo-Roman, L.A., Crosnier, C., Bartholdson, S.J., Diouf, A., Miura, K., Lambert, L.E., Ventocilla, J.A., et al. (2015). A PFRH5-Based Vaccine Is Efficacious against Heterologous Strain Blood-Stage Plasmodium falciparum Infection in Aotus Monkeys. *Cell Host Microbe* 17, 130–139.
- Payne, R.O., Silk, S.E., Elias, S.C., Miura, K., Diouf, A., Galaway, F., de Graaf, H., Brendish, N.J., Poulton, I.D., Griffiths, O.J., et al. (2017). Human vaccination against RH5 induces neutralizing antimalarial antibodies that inhibit RH5 invasion complex interactions. *JCI Insight* 2, 96381.
- Silk, S.E., Kalinga, W.F., Mtaka, I.M., Lilolime, N.S., Mpina, M., Milando, F., Ahmed, S., Diouf, A., Mkwepu, F., Simon, B., et al. (2023). Superior antibody immunogenicity of a viral-vectored RH5 blood-stage malaria vaccine in Tanzanian infants as compared to adults. *Méd.* 4, 668–686.e7.
- Jin, J., Tarrant, R.D., Bolam, E.J., Angell-Manning, P., Soegaard, M., Pattinson, D.J., Dulal, P., Silk, S.E., Marshall, J.M., Dabbs, R.A., et al. (2018). Production, quality control, stability, and potency of cGMP-produced Plasmodium falciparum RH5.1 protein vaccine expressed in Drosophila S2 cells. *NPJ Vaccines* 3, 32.
- Minassian, A.M., Silk, S.E., Barrett, J.R., Nielsen, C.M., Miura, K., Diouf, A., Loos, C., Fallon, J.K., Michell, A.R., White, M.T., et al. (2021). Reduced blood-stage malaria growth and immune correlates in humans following RH5 vaccination. *Méd.* 2, 701–719.e19.
- Silk, S.E., Kalinga, W.F., Salkeld, J., Mtaka, I.M., Ahmed, S., Milando, F., Diouf, A., Bundi, C.K., Balige, N., Hassan, O., et al. (2024). Blood-stage malaria vaccine candidate RH5.1/Matrix-M in healthy Tanzanian adults and children; an open-label, non-randomised, first-in-human, single-centre, phase 1b trial. *Lancet Infect. Dis.* [https://doi.org/10.1016/S1473-3099\(24\)00312-8](https://doi.org/10.1016/S1473-3099(24)00312-8)
- Douglas, A.D., Baldeviano, G.C., Jin, J., Miura, K., Diouf, A., Zenonos, Z.A., Ventocilla, J.A., Silk, S.E., Marshall, J.M., Alanine, D.G.W., et al. (2019). A defined mechanistic correlate of protection against Plasmodium falciparum malaria in non-human primates. *Nat. Commun.* 10, 1953.
- Foquet, L., Schafer, C., Minkah, N.K., Alanine, D.G.W., Flannery, E.L., Steel, R.W.J., Sack, B.K., Camargo, N., Fishbaugher, M., Betz, W., et al. (2018). Plasmodium falciparum Liver Stage Infection and Transition to Stable Blood Stage Infection in Liver-Humanized and Blood-Humanized FRGN KO Mice Enables Testing of Blood Stage Inhibitory Antibodies (Reticulocyte-Binding Protein Homolog 5) In Vivo. *Front. Immunol.* 9, 524.
- Brune, K.D., Leneghan, D.B., Brian, I.J., Ishizuka, A.S., Bachmann, M.F., Draper, S.J., Biswas, S., and Howarth, M. (2016). Plug-and-Display: decoration of Virus-Like Particles via isopeptide bonds for modular immunization. *Sci. Rep.* 6, 19234.
- Brune, K.D., and Howarth, M. (2018). New Routes and Opportunities for Modular Construction of Particulate Vaccines: Stick, Click, and Glue. *Front. Immunol.* 9, 1432.
- Marini, A., Zhou, Y., Li, Y., Taylor, I.J., Leneghan, D.B., Jin, J., Zaric, M., Mekhaïel, D., Long, C.A., Miura, K., and Biswas, S. (2019). A Universal Plug-and-Display Vaccine Carrier Based on HBsAg VLP to Maximize Effective Antibody Response. *Front. Immunol.* 10, 2931.
- Meireles, L.C., Marinho, R.T., and Van Damme, P. (2015). Three decades of hepatitis B control with vaccination. *World J. Hepatol.* 7, 2127–2132.
- Wright, K.E., Hjerrild, K.A., Bartlett, J., Douglas, A.D., Jin, J., Brown, R.E., Illingworth, J.J., Ashfield, R., Clemmensen, S.B., de Jongh, W.A., et al. (2014). Structure of malaria invasion protein RH5 with erythrocyte basigin and blocking antibodies. *Nature* 515, 427–430.
- Hjerrild, K.A., Jin, J., Wright, K.E., Brown, R.E., Marshall, J.M., Labbé, G.M., Silk, S.E., Cherry, C.J., Clemmensen, S.B., Jørgensen, T., et al. (2016). Production of full-length soluble Plasmodium falciparum RH5 protein vaccine using a Drosophila melanogaster Schneider 2 stable cell line system. *Sci. Rep.* 6, 30357.
- Jin, J., Hjerrild, K.A., Silk, S.E., Brown, R.E., Labbé, G.M., Marshall, J.M., Wright, K.E., Bezemer, S., Clemmensen, S.B., Biswas, S., et al. (2017). Accelerating the clinical development of protein-based vaccines for

- malaria by efficient purification using a four amino acid C-terminal 'C'-tag. *Int. J. Parasitol.* **47**, 435–446.
32. Campeotto, I., Goldenzweig, A., Davey, J., Barfod, L., Marshall, J.M., Silk, S.E., Wright, K.E., Draper, S.J., Higgins, M.K., and Fleishman, S.J. (2017). One-step design of a stable variant of the malaria invasion protein RH5 for use as a vaccine immunogen. *Proc. Natl. Acad. Sci. USA* **114**, 998–1002.
 33. Alanine, D.G.W., Quinkert, D., Kumarasingha, R., Mehmood, S., Donnellan, F.R., Minkah, N.K., Dadonaite, B., Diouf, A., Galaway, F., Silk, S.E., et al. (2019). Human Antibodies that Slow Erythrocyte Invasion Potentiate Malaria-Neutralizing Antibodies. *Cell* **178**, 216–228.e21.
 34. Douglas, A.D., Williams, A.R., Knuepfer, E., Illingworth, J.J., Furze, J.M., Crosnier, C., Choudhary, P., Bustamante, L.Y., Zakutansky, S.E., Awuah, D.K., et al. (2014). Neutralization of Plasmodium falciparum Merozoites by Antibodies against PfRH5. *J. Immunol.* **192**, 245–258.
 35. Galaway, F., Drought, L.G., Fala, M., Cross, N., Kemp, A.C., Rayner, J.C., and Wright, G.J. (2017). P113 is a merozoite surface protein that binds the N terminus of Plasmodium falciparum RH5. *Nat. Commun.* **8**, 14333.
 36. Campeotto, I., Galaway, F., Mehmood, S., Barfod, L.K., Quinkert, D., Kotraiah, V., Phares, T.W., Wright, K.E., Snijders, A.P., Draper, S.J., et al. (2020). The Structure of the Cysteine-Rich Domain of Plasmodium falciparum P113 Identifies the Location of the RH5 Binding Site. *mBio* **11**, e01566-20.
 37. Bullen, H.E., Sanders, P.R., Dans, M.G., Jonsdottir, T.K., Riglar, D.T., Looker, O., Palmer, C.S., Kouskousis, B., Charnaud, S.C., Triglia, T., et al. (2022). The Plasmodium falciparum parasitophorous vacuole protein P113 interacts with the parasite protein export machinery and maintains normal vacuole architecture. *Mol. Microbiol.* **117**, 1245–1262.
 38. Triglia, T., Scally, S.W., Seager, B.A., Pasternak, M., Dagley, L.F., and Cowman, A.F. (2023). Plasmepsin X activates the PCRRCR complex of Plasmodium falciparum by processing PfRh5 for erythrocyte invasion. *Nat. Commun.* **14**, 2219.
 39. Jamwal, A., Constantin, C.F., Hirschi, S., Henrich, S., Bildl, W., Fakler, B., Draper, S.J., Schulte, U., and Higgins, M.K. (2023). Erythrocyte invasion-neutralising antibodies prevent Plasmodium falciparum RH5 from binding to basigin-containing membrane protein complexes. *Elife* **12**, e83681.
 40. Olshefsky, A., Richardson, C., Pun, S.H., and King, N.P. (2022). Engineering Self-Assembling Protein Nanoparticles for Therapeutic Delivery. *Bioconjugate Chem.* **33**, 2018–2034.
 41. Mohsen, M.O., and Bachmann, M.F. (2022). Virus-like particle vaccinology, from bench to bedside. *Cell. Mol. Immunol.* **19**, 993–1011.
 42. Mangold, C.M., and Streeck, R.E. (1993). Mutational analysis of the cysteine residues in the hepatitis B virus small envelope protein. *J. Virol.* **67**, 4588–4597.
 43. Heppner, D.G., Jr., Kester, K.E., Ockenhouse, C.F., Tornieporth, N., Ofori, O., Lyon, J.A., Stewart, V.A., Dubois, P., Lanar, D.E., Krzych, U., et al. (2005). Towards an RTS,S-based, multi-stage, multi-antigen vaccine against falciparum malaria: progress at the Walter Reed Army Institute of Research. *Vaccine* **23**, 2243–2250.
 44. Ubillos, I., Ayestaran, A., Nhabomba, A.J., Dosoo, D., Vidal, M., Jiménez, A., Jairoce, C., Sanz, H., Aguilar, R., Williams, N.A., et al. (2018). Baseline exposure, antibody subclass, and hepatitis B response differentially affect malaria protective immunity following RTS,S/AS01E vaccination in African children. *BMC Med.* **16**, 197.
 45. Ragotte, R.J., Pulido, D., Lias, A.M., Quinkert, D., Alanine, D.G.W., Jamwal, A., Davies, H., Nacer, A., Lowe, E.D., Grime, G.W., et al. (2022). Heterotypic interactions drive antibody synergy against a malaria vaccine candidate. *Nat. Commun.* **13**, 933.
 46. Rijal, P., Elias, S.C., Machado, S.R., Xiao, J., Schimanski, L., O'Dowd, V., Baker, T., Barry, E., Mendelsohn, S.C., Cherry, C.J., et al. (2019). Therapeutic Monoclonal Antibodies for Ebola Virus Infection Derived from Vaccinated Humans. *Cell Rep.* **27**, 172–186.e7.
 47. Wrammert, J., Smith, K., Miller, J., Langley, W.A., Kokko, K., Larsen, C., Zheng, N.Y., Mays, I., Garman, L., Helms, C., et al. (2008). Rapid cloning of high-affinity human monoclonal antibodies against influenza virus. *Nature* **453**, 667–671.
 48. Jumper, J., Evans, R., Pritzel, A., Green, T., Figurnov, M., Ronneberger, O., Tunyasuvunakool, K., Bates, R., Židek, A., Potapenko, A., et al. (2021). Highly accurate protein structure prediction with AlphaFold. *Nature* **596**, 583–589.
 49. Varadi, M., Anyango, S., Deshpande, M., Nair, S., Natassia, C., Yordanova, G., Yuan, D., Stroe, O., Wood, G., Laydon, A., et al. (2022). AlphaFold Protein Structure Database: massively expanding the structural coverage of protein-sequence space with high-accuracy models. *Nucleic Acids Res.* **50**, D439–D444.
 50. Meng, E.C., Goddard, T.D., Pettersen, E.F., Couch, G.S., Pearson, Z.J., Morris, J.H., and Ferrin, T.E. (2023). UCSF ChimeraX: Tools for Structure Building and Analysis. *Protein Sci. : a publication of the Protein Society* **32**, e4792.
 51. Barrett, J.R., Pipini, D., Wright, N.D., Cooper, A.J.R., Gorini, G., Quinkert, D., Lias, A.M., Davies, H., Rigby, C., Aleshnick, M., et al. (2023). Analysis of the Diverse Antigenic Landscape of the Malaria Invasion Protein RH5 Identifies a Potent Vaccine-Induced Human Public Antibody Clonotype. Preprint at bioRxiv, 560576. <https://doi.org/10.1101/2023.10.04.560576>.
 52. Miura, K., Orcutt, A.C., Muratova, O.V., Miller, L.H., Saul, A., and Long, C.A. (2008). Development and characterization of a standardized ELISA including a reference serum on each plate to detect antibodies induced by experimental malaria vaccines. *Vaccine* **26**, 193–200.
 53. Williams, A.R., Douglas, A.D., Miura, K., Illingworth, J.J., Choudhary, P., Murungi, L.M., Furze, J.M., Diouf, A., Miotto, O., Crosnier, C., et al. (2012). Enhancing Blockade of Plasmodium falciparum Erythrocyte Invasion: Assessing Combinations of Antibodies against PfRH5 and Other Merozoite Antigens. *PLoS Pathog.* **8**, e1002991.
 54. Malkin, E.M., Diemert, D.J., McArthur, J.H., Perreault, J.R., Miles, A.P., Giersing, B.K., Mullen, G.E., Orcutt, A., Muratova, O., Awkal, M., et al. (2005). Phase 1 clinical trial of apical membrane antigen 1: an asexual blood-stage vaccine for Plasmodium falciparum malaria. *Infect. Immun.* **73**, 3677–3685.
 55. Miura, K., Zhou, H., Moretz, S.E., Diouf, A., Thera, M.A., Dolo, A., Doumbo, O., Malkin, E., Diemert, D., Miller, L.H., et al. (2008). Comparison of biological activity of human anti-apical membrane antigen-1 antibodies induced by natural infection and vaccination. *J. Immunol.* **181**, 8776–8783.
 56. Willcox, A.C., Huber, A.S., Diouf, A., Barrett, J.R., Silk, S.E., Pulido, D., King, L.D.W., Alanine, D.G.W., Minassian, A.M., Diakite, M., et al. (2021). Antibodies from malaria-exposed Malians generally interact additively or synergistically with human vaccine-induced RH5 antibodies. *Cell Rep. Med.* **2**, 100326.

STAR★METHODS

KEY RESOURCES TABLE

REAGENT or RESOURCE	SOURCE	IDENTIFIER
Antibodies		
Anti-Human IgG (g-chain specific)Alkaline Phosphatase antibody produced in goat	Sigma-Aldrich	Cat#A3188; RRID: AB_258057
Anti-Mouse IgG (whole molecule) - Alkaline Phosphatase antibody produced in goat	Sigma-Aldrich	Cat# A3562; RRID:AB_258091
Anti-Rat IgG (Whole Molecule) Alkaline Phosphatase Produced in Goat	Sigma-Aldrich	Cat# A8438; RRID:AB_258391
EBL040	Simon J. Draper, Oxford University; Rijal et al. ⁴⁶	N/A
R5.003, R5.004, R5.007, R5.008, R5.009, R5.010, R5.011, R5.013, R5.014, R5.015, R5.016, R5.017 & R5.018	Simon J. Draper, Oxford University; Alanine et al. ³³	N/A
R5.CT1	This Paper	N/A
Bacterial and virus strains		
NEB® 5-alpha Competent E. coli (High Efficiency)	New England Biolabs	Cat#C29871
Biological samples		
VAC063 Sera	Angela M. Minassian, Oxford University, ClinicalTrials.gov: NCT02927145; Minassian et al. ²¹	N/A
BALB/c Mouse Sera	This Paper	N/A
Wistar IGS Rat Sera	Noble Life Sciences, Inc. This Paper.	N/A
Chemicals, peptides, and recombinant proteins		
RH5.1	Simon J. Draper, Oxford University; Jin et al. ²⁰	N/A
RH5ΔNL	Simon J. Draper, Oxford University; Wright et al. ²⁹	N/A
RH5Nt	Simon J. Draper, Oxford University; Galaway et al. ³⁵	N/A
RH5ΔNLC-SpyTag	This Paper	N/A
RH5ΔNLC ^{HS1} -SpyTag/RH5.2-SpyTag	This Paper	N/A
HBsAg-SpyCatcher (HBsAg-SC)	Sumi Biswas, Oxford University; Marini et al. ²⁷	N/A
Hepatitis B Surface Antigen ad	BIO-RAD	Cat#PIP002
62 x 20-mer overlapping PFRH5 Peptides	Synthesized by Mimotope. Provided by Simon J. Draper, Oxford University; Payne et al. ¹⁸	N/A
Matrix-M™ Adjuvant	Novavax, Inc.	N/A
Pierce™ Diethanolamine Substrate Buffer	Thermo Fisher Scientific	Cat#34064
4-Nitrophenyl phosphate disodium salt hexahydrate	Sigma-Aldrich	Cat# N2765-100TAB; CAS:333338-18-4
Blocker Casein in PBS	Thermo Fisher Scientific	Cat#37528
StartingBlock™ T20 (PBS) Blocking Buffer	Thermo Fisher Scientific	Cat#37539
CaptureSelect™ C-tagXL Affinity Matrix	Thermo Fisher Scientific	Cat#2943072005
NHS-activated Sepharose 4 Fast Flow	Cytiva	Cat# 17090601
ExpreS ² TR reagent	ExpreS ² ion Biotechnologies/ Expression Systems	Cat# 95-055-075

(Continued on next page)

Continued

REAGENT or RESOURCE	SOURCE	IDENTIFIER
EX-CELL® 420 Serum-Free Medium for Insect Cells	Merck	Cat# 14420C-1000ML
ESF AF (Animal Free) Insect Cell Media	Oxford Expression Technologies	Cat#500400
Geneticin™ Selective Antibiotic (G418 Sulfate) (50 mg/mL)	Thermo Fisher Scientific	Cat# 10131035
Expi293™ Expression Medium	Gibco™/Thermo Fisher Scientific	Cat#A1435101
Penicillin-Streptomycin (10,000 U/mL)	Gibco™/Thermo Fisher Scientific	Cat#15140122
Critical commercial assays		
ExpiFectamine 293 Transfection Kit	Thermo Fisher Scientific	Cat#A14525
Pierce™ BCA Protein Assay Kit	Thermo Fisher Scientific	Cat#23227
Experimental models: Cell lines		
Expi293F™ cells	Thermo Fisher Scientific	Cat#A14527
ExpreS ² cells	ExpreS ² ion Biotechnologies, Denmark.	N/A
RH5.1 production cell line: <i>Drosophila melanogaster</i> Schneider 2 (S2) cell line.	ExpreS ² ion Biotechnologies, Denmark. Jin et al. ²⁰	N/A
RH5ΔNL production cell line: <i>Drosophila melanogaster</i> Schneider 2 (S2) cell line.	Simon J. Draper, Oxford University; Alanine et al. ³³	N/A
RH5ΔNLC-SpyTag & RH5.2-SpyTag production cell lines: <i>Drosophila melanogaster</i> Schneider 2 (S2) cell line	This Paper.	N/A
Experimental models: Organisms/strains		
Mice: BALB/cOlaHsd	Envigo RMS, UK.	RRID:IMSR_ENV:HSD-162
Rats: Wistar IGS, CrI:WL, Outbred	Noble Life Sciences -ordered them from Charles River (Wilmington, MA)	N/A
<i>P. falciparum</i> 3D7 clone parasites	Carole A. Long, GIA Reference Center, NIAID	N/A
Recombinant DNA		
Synthetic Genes encoding BiP-RH5ΔNLC-Linker-SpyTag-C-tag & RH5ΔNLC ^{HS1} -Linker-SpyTag-C-tag	GeneArt - Thermo Fisher Scientific	N/A
AbVec-hlg expression plasmids	Patrick C. Wilson, University of Chicago; Wrammert et al. ⁴⁷	N/A
pExpreS ² -2 <i>Drosophila</i> ExpreS ² Platform Expression plasmid	ExpreS ² ion Biotechnologies, Denmark.	N/A
Software and algorithms		
Gen5 ELISA software v3.11	Biotek, UK	N/A
GraphPad Prism version 10.0.3 for Windows	GraphPad Software Inc.	N/A
Other		
ELx800 absorbance microplate reader	Tecan	N/A
Biotek Elx808 reader	Biotek	N/A
FEI Tecnai T12 transmission electron microscope	FEI Company	N/A
ÅKTA Pure™	Cytiva	N/A
XK16 column	Cytiva	Cat#28988937
HisTrap HP His Tag	Cytiva	Cat#17524801
HiLoad 16/600 Superdex 75 pg	Cytiva	Cat#28989333
HiLoad 16/600 Superdex 200 pg	Cytiva	Cat#28989335
Superdex 200 Increase 10/300 GL	Cytiva	Cat#28990944
Superose™ 6 Increase 10/300 GL	Cytiva	Cat#29091596

RESOURCES AVAILABILITY

Lead contact

Further information and requests for resources and reagents should be directed to and will be fulfilled by the Lead Contact, Simon J. Draper (simon.draper@bioch.ox.ac.uk).

Materials availability

Matrix-M adjuvant can only be accessed via agreement with Novavax. There are restrictions to the availability of human clinical trial samples; requests should be directed to the [lead contact](#) in the first instance. All other reagents are available upon request to the [lead contact](#).

Data and code availability

- All data reported in this paper will be shared by the [lead contact](#) upon request.
- This paper does not report original code.
- Any additional information required to reanalyze the data reported in this paper is available from the [lead contact](#) upon request.

EXPERIMENTAL MODEL AND SUBJECT DETAILS

VAC063 clinical trial samples

All human serum samples were from the VAC063 clinical trial which has been reported in full elsewhere.²¹ In brief, malaria-naïve healthy UK adult volunteers received three intramuscular doses of the RH5.1 antigen²⁰ formulated in 0.5 mL AS01_B adjuvant (GSK) in various dosing regimens. Serum samples taken two weeks after the second dose or the third and final dose were used in the studies reported here. VAC063 received ethical approval from the UK NHS Research Ethics Service (Oxfordshire Research Ethics Committee A, ref. 16/SC/0345) and was approved by the UK Medicines and Healthcare products Regulatory Agency (ref. 21584/0362/001–0011). Volunteers signed written consent forms and consent was verified before each vaccination. The trial was registered on [ClinicalTrials.gov](https://clinicaltrials.gov) (NCT02927145) and was conducted according to the principles of the current revision of the Declaration of Helsinki 2008 and in full conformity with the ICH guidelines for Good Clinical Practice (GCP).

Mice

All mouse experiments were performed at the Wellcome Trust Center for Human Genetics at the University of Oxford. Six-week-old Female BALB/c mice (BALB/cOlaHsd) were purchased from Envigo, UK and housed under specific pathogen free (SPF) conditions in accordance with ARRIVE guidelines and the UK Animals (Scientific Procedures) Act 1986. Experiments were performed under Project Licence (PPL PA7D20B85) and were approved by the University of Oxford Animal Welfare and Ethical Review Body.

Rats

All rat experiments were subcontracted to Noble Life Sciences, Inc (Woodbine, MD, USA). Eight-to twelve-week-old (150–200 g) female Wistar IGS rats were ordered from Charles Rivers (Wilmington, MA, USA). All studies were conducted in compliance with the current version of the Animal Welfare Act Regulations and U.S. Public Health Service Office of Laboratory Animal Welfare (OLAW) policy on Humane Care and Use of Laboratory Animals, Guide for the Care and Use of Laboratory Animals (Institute of Laboratory Animal Resources, Commission on Life Sciences, National Research Council 1996) and AAALACi accreditation.

Cell lines

Stable Schneider 2 (S2) insect cell lines were cultured at 25°C and 125 rpm in shaker flasks with EX-CELL 420 medium (Merck) or ESF-AF medium (Oxford Expression Systems); both medias were supplemented with 100 U/mL penicillin and 100 µg/mL streptomycin (Gibco). Expi293F cells were cultured in Expi293 expression medium (Thermo Fisher Scientific) at 37°C with 8% CO₂, at a speed of 125 rpm.

METHOD DETAILS

Model of RH5.1

AlphaFold model AF-Q8IFM5-F1^{48,49} was imported into ChimeraX software⁵⁰ version 1.6.1 for visualization of the different structural regions of RH5.1.

Generation of polyclonal Schneider 2 (S2) stable cell lines

All RH5 constructs were based on the *P. falciparum* 3D7 clone sequence and potential N-linked glycosylation sequons were mutated from N-X-S/T to N-X-A. Production of stable S2 cell lines expressing the full-length RH5.1 (residues E26-Q526) and RH5ΔNL (residues K140-K247 and N297-N526) proteins has been described previously.^{20,29} Synthetic genes encoding RH5ΔNLC-ST (residues K140-K247 and N297-N506) or RH5.2-ST (residues K140-K247 and N297-N506 with 18 stabilizing mutations³²: I157L, D183E,

A233K, M304F, K312N, L314F, K316N, M330N, S370A, S381N, T384K, L392K, T395N, N398E, R458K, N463K, S467A, F505L) were codon optimized for expression in *Drosophila melanogaster* and included flanking 5' EcoRI and 3' NotI sites that were used to subclone each gene into the pExpres²-2 plasmid (Expres²ion Biotechnologies, Denmark).³⁰ These two SpyTagged RH5 constructs also included an N-terminal BiP insect signal peptide and a C-terminal flexible linker (GSGGSGGSG) followed by SpyTag (AHIVMVDAYKPTK) and C-tag (EPEA).^{25,30,31} Stable polyclonal S2 insect cells lines were generated, as previously described in detail elsewhere,³⁰ through transient transfection with Expres² TR reagent (Expression Systems) mixed with the relevant plasmid and subsequent culturing under selection with G418 (Gibco) supplemented EX-CELL 420 serum-free media (Merck).

Expression and purification of recombinant RH5 proteins

Stable monoclonal (RH5.1) or polyclonal (RH5ΔNL, RH5ΔNLC-ST, RH5.2-ST) S2 cells lines were cultured in EX-CELL 420 serum-free media (Merck) supplemented with 100 U/mL penicillin and 100 μg/mL streptomycin (Gibco) at 25°C and 125 rpm. Cell cultures were scaled up to 2.5 L and the supernatant was harvested 3 days later by centrifugation at 3,250 *xg* for 20 min followed by filtration through a 0.22 μm Steritop filter unit. Cell supernatant was then concentrated by Tangential Flow Filtration with a Pellicon 3 Ultracel 10 kDa membrane (Merck Millipore) and loaded onto a 10 mL CaptureSelect C-tagXL affinity column that had been equilibrated in Tris-buffered saline (TBS; 20 mM Tris-HCl pH 7.4, 150 mM NaCl). The column was then washed with 10 column volumes (CV) of TBS and protein eluted in 2 M MgCl₂ supplemented with 20 mM Tris-HCl pH 7.4. Eluted protein fractions were then pooled, concentrated and purified into TBS by SEC using a HiLoad 16/600 Superdex 75 or 200 pg column (Cytiva) and an ÄKTA Pure Protein Purification System (Cytiva).

The RH5-Nt protein encoded residues F25-K140 followed by rat CD4 domains 3 and 4, a biotin acceptor peptide and a C-terminal hexahistidine tag.³⁵ The protein was expressed in Expi293 cells and purified by immobilized metal affinity chromatography (IMAC) using Ni²⁺ resin followed by SEC, with protein eluted into TBS as previously described.³⁵

SDS-PAGE

Samples were prepared in 1 × Laemmli buffer with or without 50 mM dithiothreitol (Biorad). Samples were then heated for 10 min at 95°C and loaded onto a precast NuPAGE 4–12% Bis-Tris polyacrylamide gel in NuPAGE MES SDS running buffer (Thermo Fisher Scientific). Electrophoresis was performed at 200 V for 45 min and gels were stained overnight with Quick Coomassie stain (Protein Ark), destained in distilled water and imaged using an iBright FL1500 Imaging System (Thermo Fisher Scientific).

Production of anti-RH5 monoclonal antibodies

The isolation, expression and purification of the human anti-RH5 monoclonal antibodies (mAbs) used here has previously been described.³³ In brief, anti-RH5 mAbs were expressed by transient transfection of Expi293 cells with the heavy and light chain plasmids at a 1:1 ratio (0.5 μg of each plasmid per mL of culture). The supernatant was harvested 5–7 days later by centrifugation at 3,250 *xg* for 20 min, filtered through a 0.22 μm filter and then loaded onto a 5 mL Protein G HP column equilibrated in TBS. The Protein G column was washed with 10 CV of TBS and mAbs were eluted in 0.1 M glycine pH 2.7 and neutralized with Tris-HCl pH 9.0. Eluted mAbs were then buffer exchanged into TBS pH 7.4 using 30 kDa Amicon Ultra-15 centrifugal filters (Millipore).

Conjugation of RH5.2-ST to HBsAg-SC VLPs

Design, expression and purification of HBsAg VLPs with an N-terminal SpyCatcher moiety on each monomer unit (HBsAg-SC) have been previously reported in detail.²⁷ Soluble RH5.2-ST protein and HBsAg-SC VLPs were thawed on ice and supplemented with 200 mM NaCl. While on ice, 0.01–0.1 M of RH5.2-ST was added every 10 min to a fixed amount of HBsAg-SC until a final molar ratio of 1, 0.5, 0.25 or 0.1 of RH5.2-ST antigen to HBsAg-SC VLP was achieved; the reaction was then incubated overnight at 4°C. Conjugation reactions were then loaded onto a Superdex 200 10/300 Increase or Superose 6 10/300 GL Increase SEC column (Cytiva) and purified into 20 mM Tris-HCl pH 7.4, 350 mM NaCl. The SEC purification removed any free excess RH5.2-ST protein, thereby leaving the purified conjugated RH5.2-VLPs (here each VLP is now composed of a mixture of monomer units of RH5.2-ST-SC-HBsAg, i.e., those monomer units onto which the RH5.2-ST had conjugated, and also excess HBsAg-SC monomer units onto which no RH5.2-ST had conjugated). The protein concentration of the purified VLPs was measured using a Pierce BCA Protein Assay kit (Thermo Fisher). VLPs were then flash frozen in liquid nitrogen and stored at –80°C until use. Conjugation reactions were run on SDS-PAGE, and conjugation efficiency (% of HBsAg-SC monomer units in the VLP conjugated to RH5.2-ST) was assessed by densitometry.

Negative staining transmission electron microscopy (TEM)

VLPs, at 0.1 mg/mL test concentration, were adsorbed onto 200 mesh formvar/carbon copper grids for 1–2 min, washed with Milli-Q water and blotted with filter paper. Grids were then stained with 2% uranyl acetate for 10–30 s, air dried and imaged using a FEI Tecnai T12 transmission electron microscope.

Rodent immunization studies

Eight-week-old female BALB/c mice (Envigo RMS, UK) (n = 5–6 per group) were immunized intramuscularly (i.m.) with 5 μg Matrix-M adjuvant (Novavax) alone or 0.01–2 μg test antigen formulated with Matrix-M adjuvant on days 0, 21 and 42. Serum was harvested from blood collected from mouse tail veins on day 20, day 41 and by cardiac puncture on day 56. Serum was stored at –80°C.

The rat immunization study was performed at Noble Life Sciences, Inc (Maryland, USA). Female Wistar IGS rats (n = 6 per group) between 150 and 200 g (8–12 weeks old) were immunized i.m. with 2 μ g antigen formulated in 25 μ g Matrix-M adjuvant (Novavax) on days 0, 28 and 56. Serum was harvested from the blood following retro-orbital bleeding on days –2, 14, 42 and cardiac puncture on day 70. Serum samples were then frozen and shipped to the University of Oxford, UK for testing.

Monoclonal antibodies

The R5.CT1 mAb was isolated from a single IgG⁺ memory B cell in the peripheral blood mononuclear cells of an RH5.1/AS01_B human vaccinee using an RH5 probe and methodology as described in detail elsewhere.⁵¹ The antibody genes were cloned into Abvec vectors encoding the human IgG1 backbone and expressed in Expi293 cells (Thermo Fisher Scientific) by transient transfection.⁴⁷ Monoclonal antibodies were then purified from the supernatant using a HiTrap Protein A (Cytiva) affinity column followed by SEC. Production of the 2AC7, R5.016 and EBL040 mAbs has been described previously.^{33,34,46}

Monoclonal antibody ELISA

96-well flat-bottom NUNC Maxisorp plates were coated with 50 μ L (2 μ g/mL of antigen) RH5 Δ NLC-ST, RH5.2-ST or RH5.2-VLP overnight at 4°C. Plates were washed five times with PBS/Tween 20 (0.05% v/v; PBS/T) and blocked with 200 μ L Blocker Casein in PBS (Thermo Fisher Scientific) for 1 h at RT. The anti-RH5 human IgG1 mAbs used in this study have been reported previously.³³ An irrelevant human IgG1 mAb was used as a negative control. Test mAbs were added in triplicate wells at 1 μ g/mL (50 μ L/well) and plates were incubated at RT for 1 h, washed in PBS/T and then incubated with 50 μ L γ -chain specific goat anti-human IgG-alkaline phosphatase (AP) (Thermo Fisher) at a 1/2000 dilution for 1 h at RT. Plates were washed, then developed with 100 μ L *p*-nitrophenylphosphate (pNPP) (Thermo Fisher Scientific) substrate in 1 x diethanolamine buffer, read at 405 nm on an ELx800 absorbance microplate reader (Biotek) and analyzed with Gen5 software v3.11.

Standardized ELISAs

Mouse, rat or human anti-RH5.1, -RH5 Δ NL or -RH5Nt IgG ELISAs were performed on serum or purified IgG samples using a standardized methodology, as previously described.^{18,52} In brief, plates were coated with 2 μ g/mL test antigen in PBS overnight at 4°C, washed in PBS/T and blocked for 1 h at RT with 200 μ L StartingBlock or Blocker Casein in PBS (Thermo Fisher Scientific). Serum or purified IgG samples were diluted in blocking buffer, added to the plate and incubated for 1 h at RT, prior to washing and incubation with a goat anti-mouse, -rat or -human-IgG-AP secondary antibody (1:2000) for 1 h. Plates were then developed as per the mAb ELISA. Arbitrary units (AU) were assigned to the reciprocal dilution of the standard curve at which an optical density (OD) of 1 was observed. Using Gen5 ELISA software v3.11 the standard curve was used to assign AU to test samples and where possible, calibration-free concentration analysis (CFCA) was used to convert these values into μ g/mL.^{18,53}

RH5 peptide ELISAs

Methodology for ELISA using biotinylated 20-mer peptides overlapping by 12 amino acids covering the full-length RH5 sequence was reported in detail previously.¹⁸ RH5.1 and RH5-Nt protein (at 2 μ g/mL) were adsorbed to 96-well NUNC-Immuno Maxisorp plates (Thermo Fisher Scientific) and test peptides (at 10 μ g/mL) were adsorbed to streptavidin plates (Pierce) overnight at 4°C. Test purified human IgG samples and a negative pre-immunization control IgG, from VAC063 trial vaccinees,²¹ were normalized to 100 μ g/mL in Blocker Casein in PBS (Thermo Fisher Scientific) and added to triplicate wells following blocking with Blocker Casein in PBS. Blank test wells used blocking buffer only. Antibodies were detected using goat anti-human IgG-AP (Sigma) and developed and analyzed as per the mAb ELISA. The R5.CT1 human mAb was tested in the same assay at 2 μ g/mL concentration.

Anti-HBsAg endpoint ELISA

96-well flat-bottom NUNC Maxisorp plates were coated overnight at 4°C with 0.5 mg/mL recombinant HBsAg (BIO-RAD). Plates were washed with PBS/T, blocked in 5% skimmed milk and test serum samples were added in duplicate wells and diluted down the plate in a 2-fold dilution series. Following a 1 h incubation, plates were washed in PBS/T and incubated for 1 h with goat anti-mouse IgG-AP (Merck). Plates were then developed as per the mAb ELISA. Endpoint titers were calculated by determining the point at which the dilution curve intercepts the x axis at an absorbance value 3 standard deviations greater than the OD for a naive mouse serum sample.

Assay of growth inhibition activity (GIA)

GIA assays were performed according to standardized methodology from the GIA Reference Center, NIAID/NIH, as previously described.⁵⁴ In brief, total IgG was purified from serum using a 5mL HiTrap Protein-G HP (Cytiva) column and antigen-specific IgG was purified using RH5.1 or RH5 Δ NL coated resin.^{55,56} All samples were heat inactivated, depleted of anti-erythrocyte specific antibodies, buffer exchanged into RPMI-1640 media and filter sterilized prior to being incubated at varying concentrations with O+ erythrocytes and synchronized *P. falciparum* 3D7 clone trophozoites for 42 h at 37°C (“one-cycle GIA”). All samples were tested in a 2-fold dilution curve starting at a concentration of 5 mg/mL and the final parasitemia was then quantified through biochemical detection of lactate dehydrogenase in order to calculate % GIA. For the antigen reversal GIA assay, test antibodies were pre-incubated with the indicated concentration of recombinant protein, which were dialyzed against RPMI-1640, in a 96-well plate for

45 min at RT followed by a 15 min incubation at 37°C. Then, trophozoite parasites were added to the plate to start the GIA assay as described above.

QUANTIFICATION AND STATISTICAL ANALYSIS

All data were analyzed using GraphPad Prism version 10.0.3 for Windows (GraphPad Software Inc., California, USA). All tests used were two-tailed and are described in the text and/or figure legends. To analyze the GIA EC₅₀ an asymmetric logistic dose-response curve was fitted to GIA titration data with no constraints, and EC₅₀ values were interpolated. To compare ELISA or EC₅₀ values across different groups of immunized mice or rats a Kruskal-Wallis test with Dunn's multiple comparison test was performed. A value of $p < 0.05$ was considered significant.

ADDITIONAL RESOURCES

RH5.1/AS01_B (NCT02927145): <https://clinicaltrials.gov/ct2/show/NCT02927145>.

Supplemental information

Preclinical development of a stabilized RH5 virus-like particle vaccine that induces improved antimalarial antibodies

Lloyd D.W. King, David Pulido, Jordan R. Barrett, Hannah Davies, Doris Quinkert, Amelia M. Lias, Sarah E. Silk, David J. Pattinson, Ababacar Diouf, Barnabas G. Williams, Kirsty McHugh, Ana Rodrigues, Cassandra A. Rigby, Veronica Strazza, Jonathan Suurbaar, Chloe Rees-Spear, Rebecca A. Dabbs, Andrew S. Ishizuka, Yu Zhou, Gaurav Gupta, Jing Jin, Yuanyuan Li, Cecilia Carnrot, Angela M. Minassian, Ivan Campeotto, Sarel J. Fleishman, Amy R. Noe, Randall S. MacGill, C. Richter King, Ashley J. Birkett, Lorraine A. Soisson, Carole A. Long, Kazutoyo Miura, Rebecca Ashfield, Katherine Skinner, Mark R. Howarth, Sumi Biswas, and Simon J. Draper

Supplementary Figures

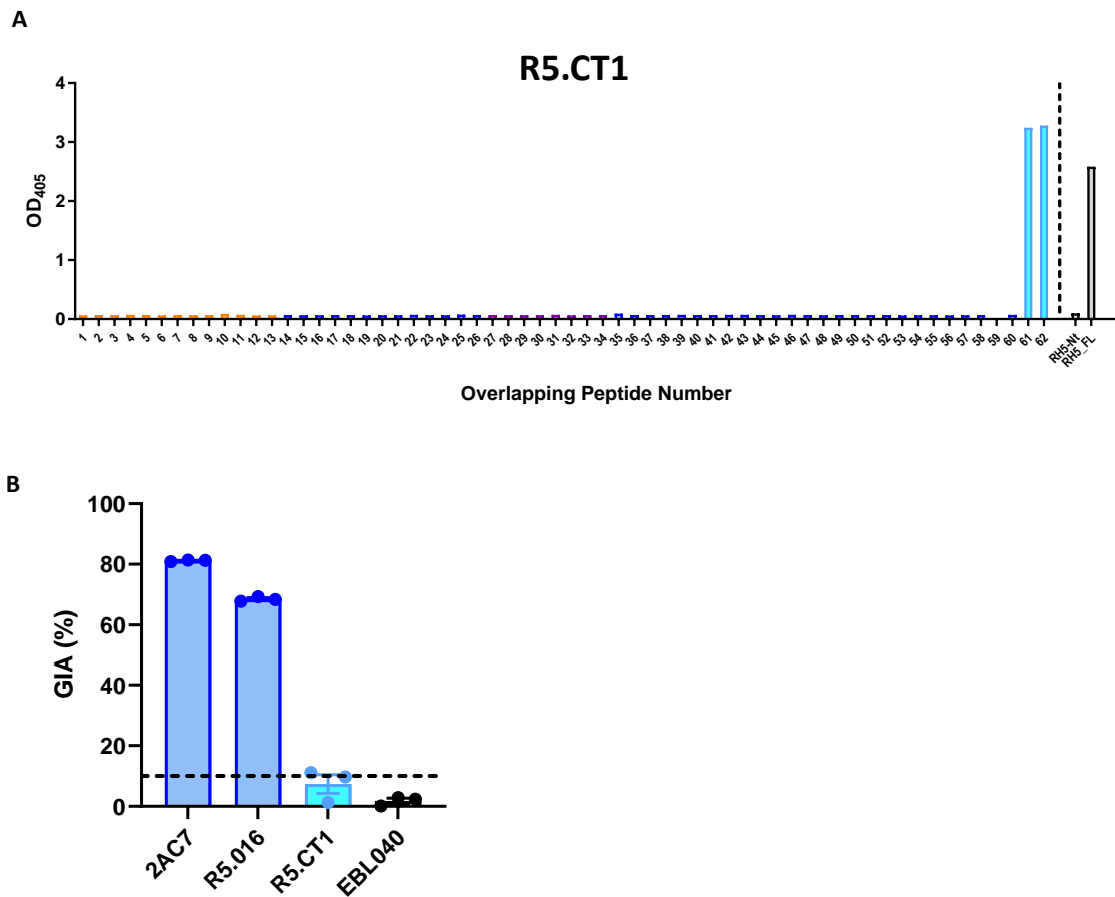


Figure S1. Assessment of an anti-RH5 C-terminal human mAb; related to Figure 1.

(A) The recombinant human IgG1 mAb, R5.CT1, was tested by ELISA at 2 μ g/mL against linear overlapping peptides spanning the RH5 vaccine insert, colour-coded as per **Figure 1**. Data from single wells are shown, but data are representative of N=3 repeats. Peptides 61 and 62 span the C-terminal 20 amino acids of RH5 and differ by only one amino acid¹. RH5-Nt and RH5_FL = recombinant protein controls for RH5 N-terminus and full-length, respectively. (B) Individual mAbs were tested in triplicate in the GIA assay against 3D7 clone *P. falciparum* parasites. Individual and mean \pm SEM GIA % are shown for each mAb. 2AC7 and R5.016 (positive control mAbs) bind RH5 Δ NL^{2,3} and were tested at 15-20 μ g/mL; EBL040 (negative control mAb against Ebola virus)⁴ and R5.CT1 were tested at 0.5 mg/mL. Dashed line at 10 % GIA represents typical cut-off for positivity in the assay.

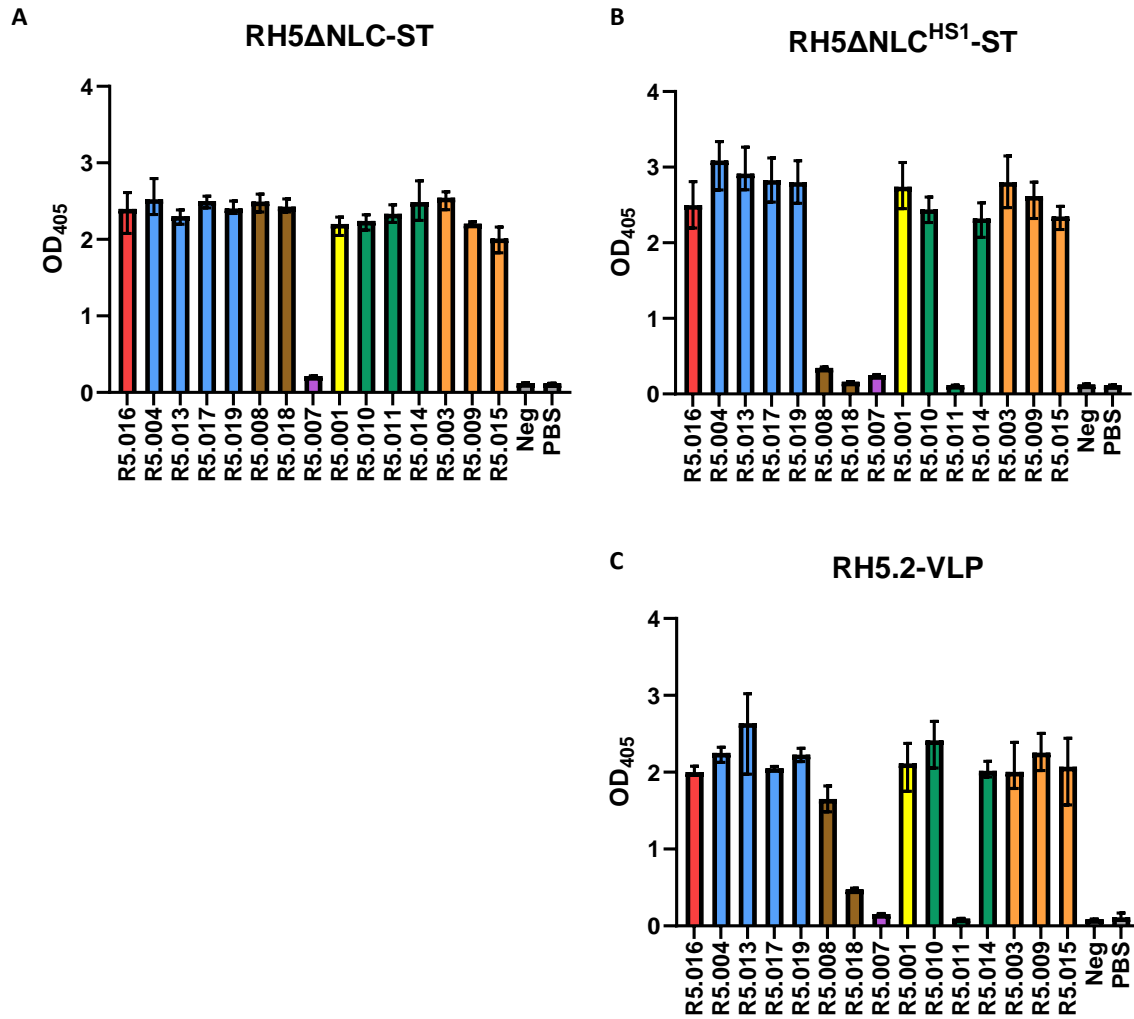


Figure S2. ELISA to screen for RH5 protein binding to a panel of anti-RH5 human mAbs; related to Figures 2 and 3.

A binding ELISA was performed on (A) RH5ΔNLC-ST protein, (B) RH5ΔNLC^{HS1}-ST protein and (C) RH5.2-VLP using a panel of anti-RH5 human mAbs. This mAb panel is color-coded as previously reported and defines seven epitope regions or antibody competition binding groups across the RH5 molecule ². Antibodies of the same color compete for binding, but do not compete with antibodies in other color-coded groups. Clone R5.007 (purple) binds a linear peptide epitope in the intrinsic loop ² and therefore should not bind to either of these proteins given they lack this sequence. The remaining six groups bind conformational epitopes ². The red, blue and brown groups include growth inhibitory antibodies that bind close to or within the basigin binding site on RH5 ²; the green antibodies do not inhibit invasion but can synergize with other growth inhibitory antibodies ²; the

yellow and orange antibodies do not inhibit parasite growth *in vitro* but block RH5 binding to CyRPA

^{2,5}. Neg is an irrelevant human IgG1 antibody control. PBS = phosphate-buffered saline only control.

Results show the mean and range of optical density at 405 nm (OD₄₀₅) of triplicate wells.

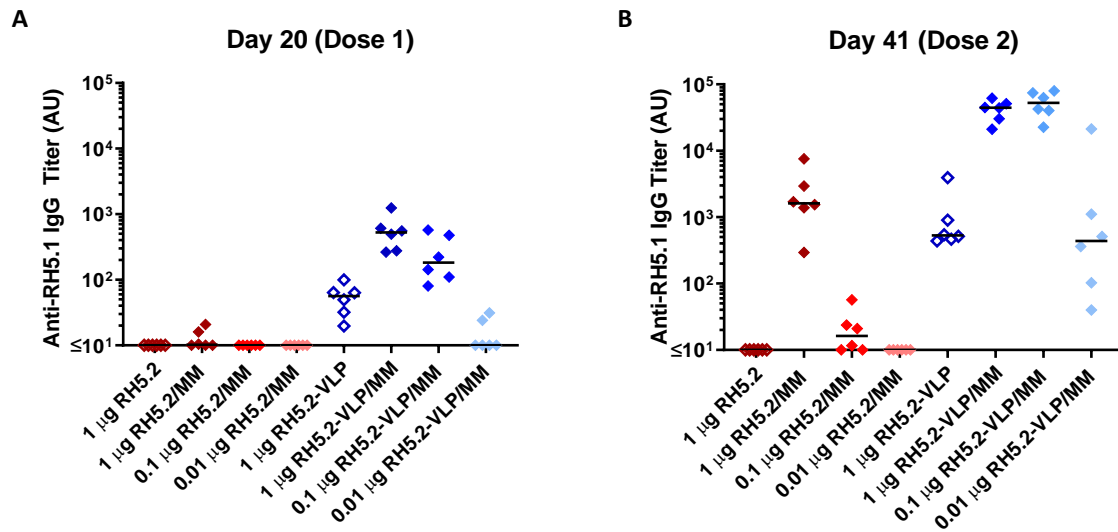


Figure S3. Immunogenicity testing of the RH5.2-VLP vaccine candidate; related to Figure 3.

BALB/c mice (N=6 per group) were immunized intramuscularly with three doses of RH5.2-ST protein or RH5.2-VLP on days 0, 21 and 42 either with (closed symbols) or without (open symbols) Matrix-M™ (MM) adjuvant. Dosing of the RH5.2-VLP was adjusted in each case to deliver the same molar amount of RH5.2 antigen as the soluble protein comparator (1, 0.1 or 0.01 µg). Anti-RH5 (full-length RH5.1) IgG titers were measured in the serum by ELISA after (A) dose 1 at day 20, and (B) dose 2 at day 41. Each point represents a single mouse and the line the median.

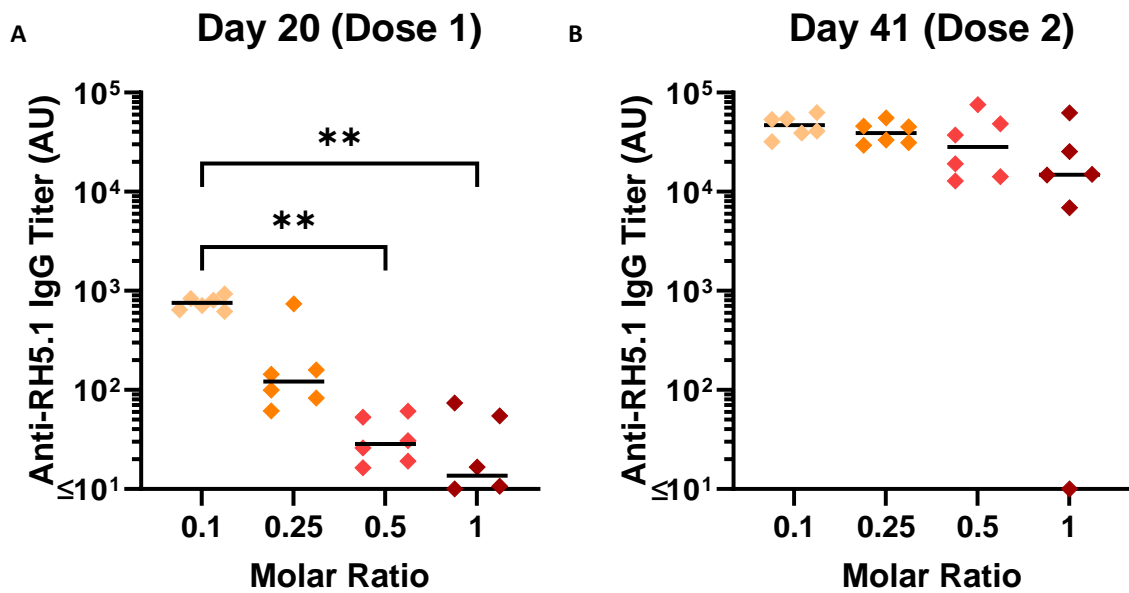


Figure S4. Immunogenicity testing of the RH5.2-VLP vaccine produced with different conjugation efficiencies; related to Figure 3.

BALB/c mice (N=6 per group) were immunized intramuscularly with three doses of RH5.2-VLP, produced using the indicated molar ratios of RH5.2-ST to HBsAg-SC (0.1:1, 0.25:1, 0.5:1 and 1:1), on days 0, 21 and 42. Dosing was adjusted in each case to deliver the same molar amount of RH5.2 antigen (10 ng); total RH5.2-VLP dose = 232, 52, 40 and 23 ng, respectively. All vaccines were formulated in Matrix-M™ adjuvant. Anti-RH5 (full-length RH5.1) IgG titers were measured in the serum by ELISA after (A) dose 1 at day 20, and (B) dose 2 at day 41. Each point represents a single mouse and the line the median. Analysis using Kruskal-Wallis test with Dunn's multiple comparison test across the four groups; ** $P < 0.01$.

Supplementary References

1. Payne, R.O., Silk, S.E., Elias, S.C., Miura, K., Diouf, A., Galaway, F., de Graaf, H., Brendish, N.J., Poulton, I.D., Griffiths, O.J., *et al.* (2017). Human vaccination against RH5 induces neutralizing antimalarial antibodies that inhibit RH5 invasion complex interactions. *JCI Insight* 2, 96381.
2. Alanine, D.G.W., Quinkert, D., Kumarasingha, R., Mehmood, S., Donnellan, F.R., Minkah, N.K., Dadonaite, B., Diouf, A., Galaway, F., Silk, S.E., *et al.* (2019). Human Antibodies that Slow Erythrocyte Invasion Potentiate Malaria-Neutralizing Antibodies. *Cell* 178, 216-228.
3. Douglas, A.D., Williams, A.R., Knuepfer, E., Illingworth, J.J., Furze, J.M., Crosnier, C., Choudhary, P., Bustamante, L.Y., Zakutansky, S.E., Awuah, D.K., *et al.* (2014). Neutralization of Plasmodium falciparum Merozoites by Antibodies against PfRH5. *J Immunol* 192, 245-258.
4. Rijal, P., Elias, S.C., Machado, S.R., Xiao, J., Schimanski, L., O'Dowd, V., Baker, T., Barry, E., Mendelsohn, S.C., Cherry, C.J., *et al.* (2019). Therapeutic Monoclonal Antibodies for Ebola Virus Infection Derived from Vaccinated Humans. *Cell Rep* 27, 172-186 e177.
5. Ragotte, R.J., Pulido, D., Lias, A.M., Quinkert, D., Alanine, D.G.W., Jamwal, A., Davies, H., Nacer, A., Lowe, E.D., Grime, G.W., *et al.* (2022). Heterotypic interactions drive antibody synergy against a malaria vaccine candidate. *Nat Commun* 13, 933.